

# **Modeling and Simulation of the Primary Reformer**



**By**

**Mohammad Ali Muzzammil**

**NUST201306015BSCME99113F**

**Nayab Nasir**

**NUST201308160BSCME99113F**

**Ahmed Kazim Fakh**

**NUST201305778BSCME99113F**

**School of Chemical and Materials Engineering**

**National University of Sciences and Technology**

**2017**

# **Modeling and Simulation of the Primary Reformer**



**By**

**Mohammad Ali Muzzammil                      NUST201306015BSCME99113F**

**Nayab Nasir    NUST201308160BSCME99113F**

**Ahmed Kazim Fakhri                              NUST201305778BSCME99113F**

**This report is submitted as FYP thesis in partial fulfillment of the  
requirement for the degree of**

**(Bachelor's in Chemical Engineering)**

**Supervisors:**

**Engr. Raheela Nawaz**

**Dr. Tayyaba Noor**

**Industrial Supervisor:**

**Mr. Tehseen Ullah Khan**

**School of Chemical and Materials Engineering (SCME)**

**National University of Sciences and Technology (NUST)**

**May, 2017**

# Certificate

This is to certify that the work in this thesis has been carried out by Mohammad Ali Muzzammil, Nayab Nasir and Ahmed Kazim Fakhri and completed under my supervision at School of Chemical and Materials Engineering, National University of Sciences and Technology, H-12, Islamabad, Pakistan.

---

**Engr. Raheela Nawaz**

Chemical Engineering  
Department  
National University of Science  
and Technology, Islamabad

---

**Dr. Tayyaba Noor**

Chemical Engineering  
Department  
National University of Science  
and Technology, Islamabad

---

**HoD: Dr. Arshad Hussain**

Department of Chemical Engineering  
School of Chemical & Materials  
Engineering, National University of  
Sciences and Technology, Islamabad

---

**Dean: Dr. Muhammad Mujahid**

Principal of School of Chemical  
and Materials Engineering ,  
National University of Sciences  
and Technology, Islamabad

## **Dedication**

The members would like to dedicate this thesis to the friends, families and teachers.

## **Acknowledgement**

The members express the gratefulness to Allah whose guidance and wisdom showed the way in all times.

The members are thankful to Engr. Raheela Nawaz and Dr. Tayyaba Noor for their efforts and guidance which allowed us to stay unwaveringly on the path.

The members are thankful to the FFC industrial supervisor, Mr. Tehseen Ullah Khan who made time from his busy schedule to aid and guide the efforts.

Finally, the members are thankful to all the faculty members of the institution for instilling within the fundamental principles of engineering which provided valuable help.

**Abstract:**

The Primary Reformer is an integral unit of the ammonia synthesis plant. Ammonia is reacted with Carbon dioxide to create Urea fertilizer. And for the production of Ammonia, Hydrogen needs to be produced through the formation of syngas. The reformer is a packed tubular bed reactor with Ni-based catalyst. The volume of the chamber is 40 m<sup>3</sup>. Operating conditions are 600 °C and 36 kg/cm<sup>2</sup>g for the feed and 808 °C and 32 kg/cm<sup>2</sup>g for the exit with the burners operating at 1015 °C being fed fuel at 35 °C.

There are two main reactions occurring in the reformer:



The above reaction is endothermic and is the major reaction taking place in the reformer, with an extent more than twice that of the second. This is the methane steam reforming.

The second reaction is exothermic which provides some of the heat requirement of the first endothermic reaction. This is the water gas shift reaction.



The rest of the heat for the convective part of the primary reformer is provided by the radiant section. The heat in the primary reformer is supplied by combustion of natural gas in burners inside the reformer. The exhaust flue gases exit through the chimney after waste heat recovery.

## Table of Contents:

Certificate.....	i
Acknowledgement.....	iii
Abstract:.....	iv
Chapter 1: Introduction.....	1
1.1. Introduction: .....	1
1.2. Scope of the Project: .....	2
1.3. Process Description: .....	2
1.4. Process Flow Diagram .....	4
Chapter 2: Literature Review .....	5
Microchannel methane steam reformers with improved heat transfer efficiency and their long-term stability by Min-Ho Jin et al.....	5
The kinetics of methane steam reforming over a Ni/a-Al <sub>2</sub> O catalyst by Kaihu Hou and Ronald Hughes. ....	8
Mathematical modelling of methane steam reforming in a membrane reactor: an isothermic model E.M. Assaf, C.D.F. Jesus and J.M. Assaf .....	15
Methane/steam global reforming kinetics over the Ni/YSZ of planar pre-reformers for SOFC systems by Van Nhu Nguyen et al.....	18
Chapter 3: Methodology .....	23
3.1. Material Balance: .....	23
3.2. Energy Balance:.....	30
3.2.1. Fuel Mixing Point:.....	31
3.2.2. Burner Balance: .....	32
3.2.3. Reformer Energy Balance: .....	34
3.2.4. Summarized Energy Balance: .....	34
3.3. Simulation: .....	35
3.4. HAZOP analysis .....	46
3.5. Costing: .....	48
3.5.1. Reactor Cost: .....	48
3.5.2. Cost of Hydrogen-Desulphurization Tank:.....	49
3.5.3. Heat Exchanger Costing:.....	50
3.5.4. Raw Material Cost: .....	51
Variable Cost and Fixed Cost:.....	51
3.5.5. Variable Cost: .....	52
3.5.6. Fixed Costs:.....	52

<b>Chapter 4: Results and Discussions</b> .....	<b>53</b>
<b>Conclusion</b> .....	<b>60</b>
<b>References</b> .....	<b>61</b>
<b>Appendices</b> .....	<b>66</b>
<b>Appendix A.1</b> .....	<b>66</b>
<b>Appendix A.2</b> .....	<b>74</b>
<b>Nomenclature:</b> .....	<b>81</b>



## List of Tables:

<b>Table 1: Experimental conditions.....</b>	<b>9</b>
<b>Table 2: Reaction equations and equilibrium constants .....</b>	<b>11</b>
<b>Table 3: Parameter estimates for final model .....</b>	<b>13</b>
<b>Table 4: Activation energies, adsorption enthalpies and other factors.....</b>	<b>14</b>
<b>Table 5: Inlet stream to reformer .....</b>	<b>26</b>
<b>Table 6: Stream compositions and parameters.....</b>	<b>27</b>
<b>Table 7: Reformers material balance .....</b>	<b>29</b>
<b>Table 8: Fuel mixing point .....</b>	<b>31</b>
<b>Table 9: Furnace balance .....</b>	<b>33</b>
<b>Table 10: HAZOP analysis of furnace .....</b>	<b>47</b>
<b>Table 11: HAZOP analysis of reformer .....</b>	<b>47</b>
<b>Table 12: Variable and fixed costs methodology .....</b>	<b>51</b>
<b>Table 13: Variable costs .....</b>	<b>52</b>
<b>Table 14: Fixed costs.....</b>	<b>52</b>
<b>Table 15: Industrial and calculated results comparison .....</b>	<b>53</b>
<b>Table 16: Dry basis composition comparison.....</b>	<b>54</b>
<b>Table 17: Conversion of reactions .....</b>	<b>55</b>
<b>Table 18: Calculated and simulated results.....</b>	<b>55</b>
<b>Table 19: Error reduction .....</b>	<b>56</b>
<b>Table 20: Calculated, simulated and industrial results comparison .....</b>	<b>57</b>
<b>Table 21: HAZOP analysis of furnace .....</b>	<b>59</b>
<b>Table 22: HAZOP analysis of reformer .....</b>	<b>59</b>

## List of Figures:

Figure 1:Diagram of Case A, lateral burning and Case B, top burning.....	6
Figure 2: Conversion of methane vs selectivity of carbon dioxide .....	10
Figure 3: Exemplary product compositions of dry gaseous species Hydrogen and Methane at different volumetric flow rates as a function of S/C=2.5 .....	21
Figure 4: Block diagram for balances .....	24
Figure 5: Step 1 for simulation .....	36
Figure 6: List of components .....	37
Figure 7: Property method selection .....	37
Figure 8: Properties input complete.....	38
Figure 9: Reaction definition .....	39
Figure 10: Reactions properly defined.....	39
Figure 11: Stoichiometric coefficients for SMR .....	39
Figure 12: Kinetics for SMR .....	40
Figure 13: Kinetics for WGS.....	40
Figure 14: Reformer flowsheet .....	41
Figure 15: Reaction specifications .....	42
Figure 16: Possible reactants. ....	43
Figure 17: Molar extents defined.....	43
Figure 18: Specifications for WGS .....	44
Figure 19: Flowsheet with reformer and furnace .....	45
Figure 20: Overall flowsheet .....	46
Figure 21: Table of conditions and compositions of simulation .....	57
Figure 22: Cv and Percentage opening .....	58
Figure 23: Xt and Percentage opening.....	58
Figure 24: Fl and Percentage opening.....	58

# Chapter-1

## Introduction

### 1.1. Introduction:

Primary reformer is an essential part of the Urea production process. The reformer produces Syngas, which is hydrogen and carbon monoxide. The reforming process is the first major step and the first unit of the Ammonia process plant.

Nitrogen and hydrogen are required for the production of ammonia gas which is essential in the further downstream production of urea and nitrogenous fertilizers. The nitrogen for the reaction is taken in in the form of air which reacts with hydrogen. The hydrogen gas though, unavailable in the air, can either be produced through the electrolysis of water or through steam reforming of methane or natural gas. Keeping in hindsight the economics of the process, the production of hydrogen through reforming of natural gas, comprised mainly of methane. The gas is input into the reformer where steam is injected into the tubes co-currently. The tubes are lined with nickel catalyst on the surface of calcium oxide/aluminum oxide support. In the case of FFC, it the aluminium support. The tubes are made up of nickel alloy tubes to withstand high pressure and temperature. The process is an endothermic one hence large amounts of heat is required to favor the forward reaction.

High temperatures and low pressures favor the formation of the products according to the Le Chatelier's Principle. The reactants are passed over a catalyst of nickel, based on the surface of a calcium oxide/aluminium oxide support contained in vertical nickel alloy tubes. The tubes, 180 in parallel, are heated in a furnace at high temperatures and pressures.

## **1.2. Scope of the Project:**

The scope of the project is to model and simulate the primary reformer section in the FFC plant at Goth Machhi. The FFC Goth Machhi Plant is one of the largest fertilizer producing plants in the country. The simulation and project is based on the Plant-2 of the ammonia producing plant.

There have been some drop in outputs from Plant-2 due to different reasons. The FFC management wants to model and simulate their Plant-2 primary reformer. The simulation results are also to be compared with the results obtained through the plant and discrepancies compared between the two to look for possible solutions to the plant's problems.

## **1.3. Process Description:**

This process is for generation of ammonia which is an important component for production of the urea based fertilizers in FFC.

The natural gas is supplied to the plant through Mari gas-field and enters the battery limit. A flow meter is attached here which records the value of the gas flow intake to the plant. This is natural gas from Mari which is to be converted into hydrogen and carbon dioxide gas.

The gas first comes and passes through a heat exchanger as heats up by the heat exchange with recycled gas. It then travels to the knock-out drum.

The knock out drum acts as a flashing device. It flashes the gas vapors coming from the battery limit and the liquid portion condenses down into the flash tank. It is basically binary separation. This is an important step, otherwise the oxides of carbon which are present may react with the moisture to form carbonic acid which would result in corrosion for the downstream processing metallurgy. The tank is stainless steel tank and cylindrical in shape to sustain the high pressures. A compressor is also added in the loop which compresses instrument air for use in the process downstream.

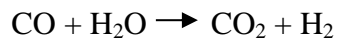
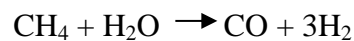
After the flash tank, the gas travels to the desulphurizer unit. This unit is quite important in the sense that sulphur impurities downstream in primary and secondary reformer can poison the catalyst. The desulphurizer unit has beds which adsorb the

trace amounts of sulphur in the gas before it is sent down stream. The beds are of zinc oxide pellets placed on a mesh. It reacts with the gas and absorbs and accumulates the sulphur impurities. The beds in the desulphurizer have to be re-generated with time, usually after two years.

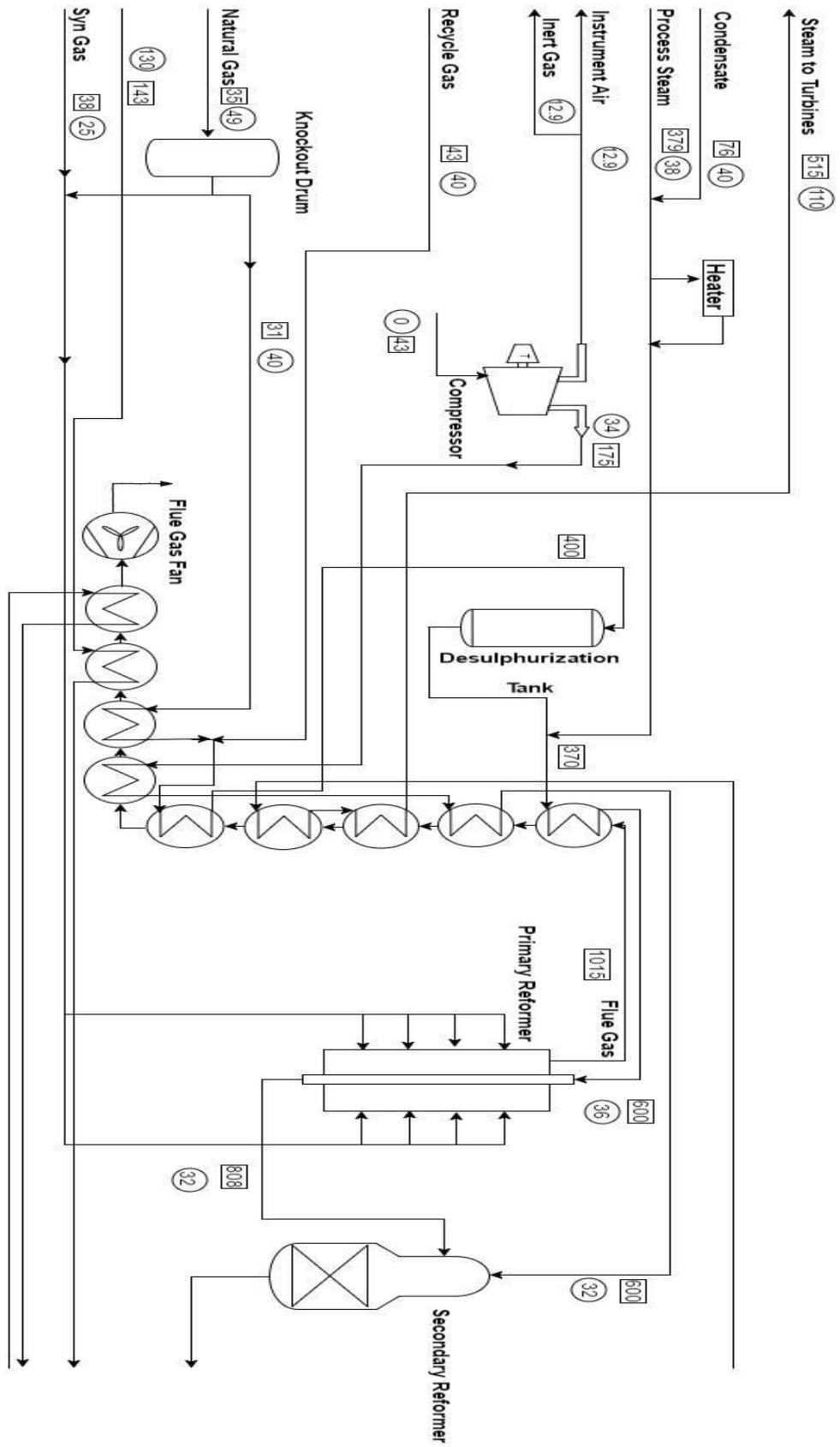
The processed gas then passes on to a series of heat exchangers where heat exchange takes place between flue gases and the recycle gas to heat up the gas before injecting it in the reformer. The heat exchangers are all shell and tube heat exchangers with a large continuous shell which is the chimney and housing tubes of different lengths and diameters containing different fluids to ensure there is no wastage of energy. They are also single pass shell and tube. The process gas heater heats the feed stream to the reformer. The super steam heater heats up the steam which has been brought in through boilers. Steam is important component of the SMR reaction. The process gas enters the reformer from the top after going through the heater.

The reformer is a furnace like structure which contains tubes containing catalyst beads. There are 180 tubes in the primary reformer. The gas passes through the tubes and hydrogen gas, carbon dioxide, carbon monoxide and water are produced from these following set of reactions. The catalyst used in the tubes is basically Nickel based catalyst based on alumina support. The nickel based catalyst is quite expensive and is susceptible to fouling or poisoning by sulphur impurities.

The reactions taking place in the reformer are the methane steam reforming and the water gas shift reaction the reactions of which are listed below, respectively.



# 1.4. Process Flow Diagram



# Chapter-2

## Literature Review

The literature consulted, revolved primarily around research papers. Kinetics were studied, the modelling and the future prospects in steam reforming and compiled them as concisely as the members could without leaving out important parts of the study. They are arranged in chronological order.

The first paper studied was *Microchannel methane steam reformers with improved heat transfer efficiency and their long-term stability* by Min-Ho Jin *et al.*

The paper helped with understanding the importance heat transfer plays in the conversion of methane in the reaction.

This research paper deals, primarily, with improving the heat transfer efficiency from the radiant section to the catalyst contained within the convective section where the primary reactions the members deal with in this project take place. It is stated that the efficiency is more important to the industry than the reaction activity. Microchannel are famed for their high heat transfer rate, applied to both the combustion reaction and the reforming reaction taking place. The study improved the heat transfer efficiency by utilizing a porous membrane type catalyst. Their findings resulted in a 14.7% increase in methane conversion.

MCRs have quite recently revealed good performance [1]. The research focused with Cu50/Zn50 (Ce5) catalyst. Peela *et al.*[2]used a Rh/CeO<sub>2</sub>/Al<sub>2</sub>O<sub>3</sub> catalyst for ethanol steam reforming. However, the most widely used catalysts have been nickel-based [3-7].

The paper differentiates itself from these on the basis that these research papers used a powder-type catalyst whereas here it would be a poor choice as they would not improve the heat transfer efficiency. The paper reiterates the findings of the previous studies [8-10] where a porous membrane type catalyst was used for higher efficiencies.

The study moves onwards with a detailed mention about the fabrication of the catalysts which are Nickel based oxides in the form of porous membranes. Abridged,

the Nickel was wet impregnated with Pd and Al<sub>2</sub>O<sub>3</sub> and was then pretreated with 90% H<sub>2</sub>, 10% Ar at 450°C to remove any organics. After being pressurized, the powder adopted the form of a membrane and was then thermally treated at 1100°C with H<sub>2</sub> for improving the mechanical strength.

Furthermore, the fabrication of the MCR was then addressed. Etched patterns of INCOLOY 800TH plates were used (200mm x 60mm x 1mm with 0.5 mm etching). Essentially, the MCR is a membrane which acts as the catalyst and 30 micro-channel plates which are categorized as mixing plates, separating plates, catalyst plates, reactant in-flow plates, product out-flow plates, burner plates, heat exchanging plates and cover plates.

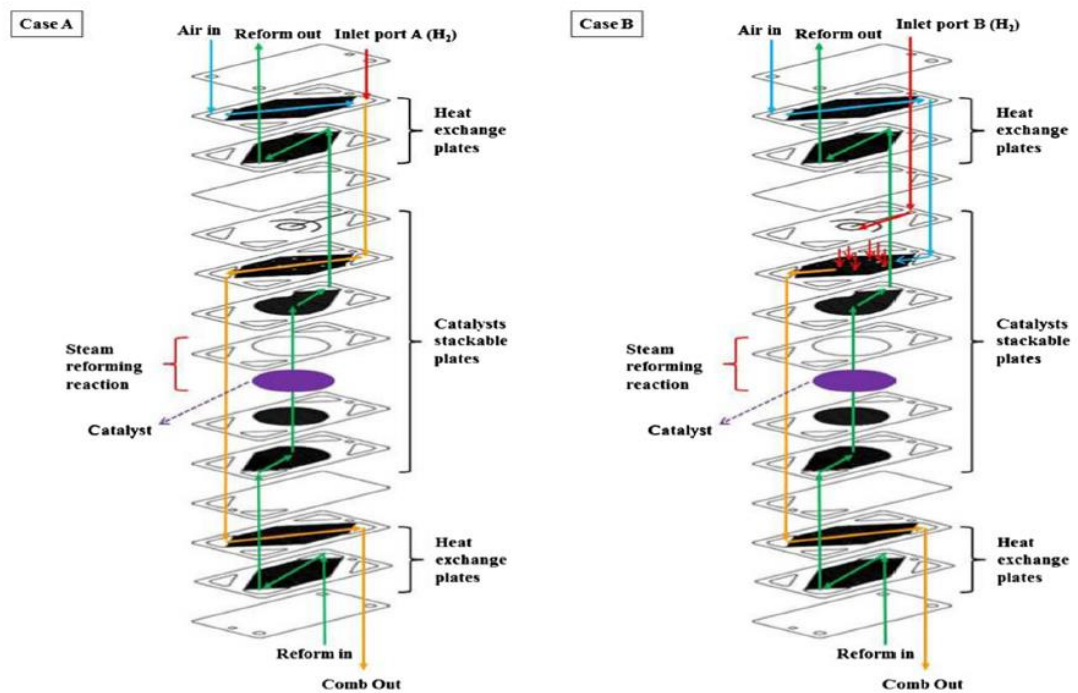


Figure 1: Diagram of Case A, lateral burning and Case B, top burning

Steam and methane move downwards through the micro-channel reactor and air and hydrogen and the rest of the products move counter-currently and therefore upwards. This is done for making the heat exchange between the hot products and the cold reactants more efficient and to preheat the reactants entering the catalyst chamber. Moisture is then removed from the products using a cold trap and the quantitative analysis of the products is done by gas chromatography. Temperature was noted by 5 k-type thermocouples. The steam to carbon ratio used was 3 under atmospheric



pressure and gaseous space velocity was 10,000/h. The feed flow rates of hydrogen and air were 3159 ml/min at 1 bar and 1327 ml/min at 1.4 bar respectively.

The total pore volume for the catalyst was 0.0806 mL/g with the average pore diameter for the catalyst equal to 388.8 nm and 39.9% porosity.

Two entry points for hydrogen A and B were positioned. This was done to vary the location of the combustion region. Hydrogen is fed to the MCR at inlet port A and is used as a combustion product on the lateral side of the catalyst. For B, hydrogen is supplied at inlet port B which makes its combustion point positioned above the membrane catalyst.

The findings of the study were that the temperature difference for case A was around 500°C. Hot spots were also noticed which would lead to thermal failure and poor longevity of the MCR. Longevity is highly important to the industry.

For case B, the verdict was much more precise. The temperature difference was reduced to 150°C which meant that moving the combustion point to the top, as opposed to the side, of the catalyst improved heat transfer. Case B also provided a higher methane conversion, 86.6% as opposed to 71.9% of case A, and case B reduced methane slippage of 3.2% compared to 7.8% for case A. It was also noted that both the mechanical and long-term stability of case B were also considerably higher than case A's.

Hydrogen permeation rate increased with increasing pressure difference between the surroundings and the catalyst surface. The H<sub>2</sub>/N<sub>2</sub> selectivity of the catalyst was observed to increase as the pressure difference changed, this was a linear relationship.

Finally, the study concluded its findings. The efficiency of heat transfer was increased by making use of a porous membrane catalyst and moving the combustion point from the side of the catalyst to the top. This caused a 14.7% increase in methane conversion this high performance continued for up to 500 hours.

Although akin to secondary reforming the effects of using a membrane type catalyst are clearly depicted in this study which comprehensively highlights the trend the industry should take in the future.

Next onwards to studying the kinetics and came across a well-constructed paper *The kinetics of methane steam reforming over a Ni/a-Al<sub>2</sub>O catalyst* by Kaihu Hou and Ronald Hughes.

This paper proved useful for the kinetics for the methane steam reforming and the water gas shift reaction. There is a direct relationship between the rate of disappearance and partial pressures of methane. The kinetic rate being used were the Langmuir Hinshelwood Hougen Watson equations. Another new concept learned was the Freundlich's adsorption methodology.

In the intro of the paper a plethora of papers is found involving the kinetics each adding to the other preceding ones [11-20].

Now the concept of establishing a mathematical model of the entire steam reforming process is of particular complexity as there are several reactions occurring, either in series or in parallel, dependent on a variety of variables.

The multitude of mechanisms and kinetics owing to this process are due to the reasons that changing the catalyst composition results in changes in the parameters and that the limits applied to the understanding of diffusion of this process are due to a poor comprehension of the mechanisms of kinetics [21].

Therefore the establishing of a general kinetic equation is impossible. It is for this reason why the mechanism and kinetics are different for each and every different iteration of steam reforming with different mass and heat transfers alongside the diffusion rates.

The paper states that there are two sorts of kinetic equations, the first is based on the rate of disappearance of methane [11,14,15,22-25] and the second is primarily for the rate of formation of either of the substances, carbon monoxide or carbon dioxide [17,19,20,26,27]. The second type proves more valuable as it provides an extensively detailed variation of operation conditions to be used for the required conversion.

The paper analyzed the thermodynamics of the reaction and used the Langmuir Hinshelwood Hougen Watson methodology and Freundlich's adsorption concept.

The paper then proceeds with an account of catalyst pretreatment and preliminary experiments of the primary purpose to simply find out the rate of catalyst deactivation. This was useful for the paper to ensure the stability of the catalyst. Under lower temperatures and higher pressures with not a very high steam to carbon ratio, the catalyst deactivated quickly because of carbon deposition on its surface [28].

Therefore, the smaller the size of the catalyst, the higher the chance that it may deactivate quickly. The paper also mentions that to ensure less carbon deposition on the catalyst, a fraction of hydrogen produced can be incorporated to the feed stream to increase the hydrogen to carbon ratio. Total pressure was 120 kPa,  $W / F_{CH_4}$  was 13356 kg cat s/kmol. The molar ratios of  $H_2O:CH_4:H_2$  were 5.5:1:1 for the feed and temperature was 798 K and 823 K for different iterations of the reactions.

The conditions for the water gas shift were a total pressure of 120 kPa,  $W / F_{CO_2}$  was 13356 kg cat s/kmol with a hydrogen to carbon dioxide molar ratio of 0.75:1 at 673 K.

The high hydrogen to carbon ratio of the experiment which was significantly higher than commercial ratios was noticed.

The experiment noted that there was no significant change to conversion when the catalyst particle size becomes smaller than 0.15 mm. This is because at these small sizes, intra-particle diffusion resistance and film resistance are infinitesimally low.

Table 1: Experimental conditions

Experimental conditions		
Pressure (kPa)	Temperature (K)	$H_2O:CH_4:H_2$ molar ratio
Methane steam reforming experiments		
120	748, 773, 798, 823	4:1:1
120	748, 773, 798, 823	5.5:1:1
300	748, 773, 798, 823	5.5:1:1
450	798, 823	5.5:1:1
600	748, 773, 798, 823	5.5:1:1
120	748, 773, 798, 823	7:1:1
Reverse water gas shift experiments		$H_2/CO_2$ (molar ratio)
120	598, 623, 648, 673	0.75
120	598, 623, 648, 673	0.5

The temperature effect on conversion is a non-linear relationship and that at low methane concentrations the relationship between conversion and contact time is

proportional. The higher the steam:methane ratio, the longer is the range of this proportionality trend between conversion and contact time. A correlation of methane disappearance and partial pressure of methane was found to be linear as long as the methane concentration was low.

The paper then moves towards carbon dioxide selectivity which is essentially the ratio of moles of  $\text{CO}_2$  to  $\text{CH}_4$ . This helps determine the product composition. It was noted that selectivity decreases linearly with increasing conversion. Why this happens is because carbon dioxide is converted by the water gas shift reaction back to carbon monoxide.

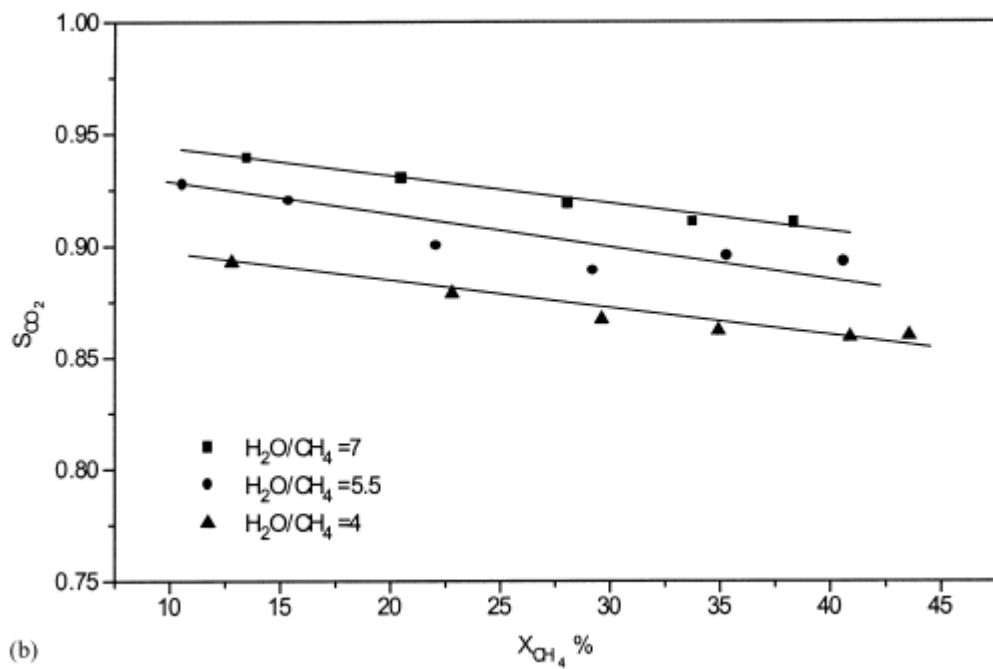


Figure 2: Conversion of methane vs selectivity of carbon dioxide

An example of the trend of selectivity vs methane conversion is depicted above.

Now the paper discusses the topics most important, the thermodynamic analysis.

Table 2: Reaction equations and equilibrium constants

<i>I</i>	Reaction	$K_{p_i}$	Dimensions
1	$\text{CH}_4 + \text{H}_2\text{O} = \text{CO} + 3\text{H}_2$	$1.198 \times 10^{17} \exp(-26830/T)$	$(\text{kPa})^2$
2	$\text{CO} + \text{H}_2\text{O} = \text{CO}_2 + \text{H}_2$	$1.767 \times 10^{-2} \exp(4400/T)$	$(\text{kPa})^0$
3	$\text{CH}_4 + 2\text{H}_2\text{O} = \text{CO}_2 + 4\text{H}_2$	$2.117 \times 10^{15} \exp(-22430/T)$	$(\text{kPa})^2$
4	$\text{CH}_4 + \text{CO}_2 = 2\text{CO} + 2\text{H}_2$	$6.780 \times 10^{18} \exp(-31230/T)$	$(\text{kPa})^2$
5	$\text{CH}_4 + 3\text{CO}_2 = 4\text{CO} + 2\text{H}_2\text{O}$	$2.170 \times 10^{22} \exp(-40030/T)$	$(\text{kPa})^2$
6	$\text{CH}_4 = \text{C} + 2\text{H}_2$	$4.161 \times 10^7 \exp(-10614/T)$	kPa
7	$2\text{CO} = \text{C} + \text{CO}_2$	$5.744 \times 10^{-12} \exp(20634/T)$	$(\text{kPa})^{-1}$
8	$\text{CO} + \text{H}_2 = \text{C} + \text{H}_2\text{O}$	$3.173 \times 10^{-10} \exp(16318/T)$	$(\text{kPa})^{-1}$
9	$\text{CO}_2 + 2\text{H}_2 = \text{C} + 2\text{H}_2\text{O}$	$1.753 \times 10^{-8} \exp(12002/T)$	$(\text{kPa})^{-1}$
10	$\text{CH}_4 + 2\text{CO} = 3\text{C} + 2\text{H}_2\text{O}$	$4.190 \times 10^{-12} \exp(22022/T)$	$(\text{kPa})^{-1}$
11	$\text{CH}_4 + \text{CO}_2 = 2\text{C} + 2\text{H}_2\text{O}$	$0.730 \exp(1388/T)$	$(\text{kPa})^0$

The first is methane steam reforming reaction and the second is the water gas shift reaction. The focus is mainly directed towards these. The first reaction increases monotonically with the extent of reaction in the forward direction. The second reaction is quite reversible.

Next towards how pressure and steam:methane ratio effect the rates of reaction and in this section the paper discusses the steps that take place during the reaction about how reactants absorb to the surface of the catalyst either with or without dissociation, how reaction occurs on the surface of the catalyst and how the products desorb from the surface. The paper then proceeds with experiments on as to which of these is the rate determining step.

Finding the relation between conversion and time in the paper as follows:

$$X_{\text{CH}_4} = a_0 + a_1 \left( \frac{W}{F_{\text{CH}_4}} \right) + a_2 \left( \frac{W}{F_{\text{CH}_4}} \right)^2 + a_3 \left( \frac{W}{F_{\text{CH}_4}} \right)^3 \quad (3)$$

$$X_{\text{CO}_2} = b_0 + b_1 \left( \frac{W}{F_{\text{CH}_4}} \right) + b_2 \left( \frac{W}{F_{\text{CH}_4}} \right)^2 + b_3 \left( \frac{W}{F_{\text{CH}_4}} \right)^3 \quad (4)$$

By putting in the values of the variables  $a_i$  and  $b_i$  the conversion with respect to time is easily identifiable.

$$r_{\text{CH}_4} = \frac{dX_{\text{CH}_4}}{d(W/F_{\text{CH}_4})} = a_1 + 2a_2 \left( \frac{W}{F_{\text{CH}_4}} \right) + 3a_3 \left( \frac{W}{F_{\text{CH}_4}} \right)^2 \quad (5)$$

$$r_{\text{CO}_2} = \frac{dX_{\text{CO}_2}}{d(W/F_{\text{CH}_4})} = b_1 + 2b_2 \left( \frac{W}{F_{\text{CH}_4}} \right) + 3b_3 \left( \frac{W}{F_{\text{CH}_4}} \right)^2 \quad (6)$$

Rates of formation of carbon dioxide and usage of methane.

From this point, it can now be calculated, the rate of reaction for the water gas shift reaction.

$$\begin{aligned} r^{\bullet} \text{CO}_2 &= \frac{dX^{\bullet} \text{CO}_2}{d(W/F_{\text{CO}_2})} \\ &= a^{\bullet} 1 + 2a^{\bullet} 2 \left( \frac{W}{F_{\text{CO}_2}} \right) + 3a^{\bullet} 3 \left( \frac{W}{F_{\text{CO}_2}} \right)^2 \\ r^{\bullet} \text{CH}_4 &= \frac{dX^{\bullet} \text{CH}_4}{d(W/F_{\text{CO}_2})} \\ &= b^{\bullet} 1 + 2b^{\bullet} 2 \left( \frac{W}{F_{\text{CO}_2}} \right) + 3b^{\bullet} 3 \left( \frac{W}{F_{\text{CO}_2}} \right)^2 \end{aligned}$$

The rate of methane disappearance decreased as the ratio of steam to methane was increased because the partial pressure of methane was reduced because of the increasing ratio [11, 15, 20, 25, 29]. Another reason to explain this is that the high amount of steam hinders the absorption rate of methane from the catalyst surface.

The article now started on the model development, an area of incredible importance particularly because of the mechanisms and rate equations. But the most important piece of the article was the kinetic mechanism on which the simulation was based.

There were 5 assumptions to the model which were:

- Steam reacts on the nickel catalyst's surface dissociating into hydrogen and oxygen atoms.
- Methane reacts on the surface of the nickel catalyst producing CH<sub>2</sub> and hydrogen atoms.

- CH<sub>2</sub> and oxygen radicals then proceed to react and produce CHO and hydrogen atoms.
- CHO then dissociates to produce CO and H and further may react with oxygen atoms to produce CO<sub>2</sub>.
- CO reacts with oxygen in the catalyst's surface to produce CO<sub>2</sub> and then desorbs to the gas phase.

Ultimately, these are the kinetic rate equations for methane steam reforming and water gas shift reaction:

$$r_1 = \frac{k_1(P_{\text{CH}_4} P_{\text{H}_2\text{O}}^{0.5} / P_{\text{H}_2}^{1.25})(1 - (P_{\text{CO}} P_{\text{H}_2}^3 / K_{p1} P_{\text{CH}_4} P_{\text{H}_2\text{O}}))}{(\text{den})^2} \quad (14)$$

$$r_2 = \frac{k_2(P_{\text{CO}} P_{\text{H}_2\text{O}}^{0.5} / P_{\text{H}_2}^{0.5})(1 - (P_{\text{CO}_2} P_{\text{H}_2} / K_{p2} P_{\text{CO}} P_{\text{H}_2\text{O}}))}{(\text{den})^2} \quad (15)$$

$$r_3 = \frac{k_3(P_{\text{CH}_4} P_{\text{H}_2\text{O}} / P_{\text{H}_2}^{1.75})(1 - (P_{\text{CO}_2} P_{\text{H}_2}^4 / K_{p3} P_{\text{CH}_4} P_{\text{H}_2\text{O}}^2))}{(\text{den})^2} \quad (16)$$

Den here is equal to  $1 + K_{\text{CO}} P_{\text{CO}} + K_{\text{H}} P_{\text{H}_2\text{O}} / P_{\text{H}_2} + K_{\text{H}_2\text{O}} (P_{\text{H}_2\text{O}} / P_{\text{H}_2})$

Table 3: Parameter estimates for final model

Temperature (K)	$k_1 \times 10^7$ (kmol/ kg cats (kPa) <sup>0.25</sup> )	$k_2 \times 10^5$ (kmol/ kg cats (kPa))	$k_3 \times 10^6$ (kmol/ kg cats (kPa) <sup>0.25</sup> )	$K_{\text{CO}} \times 10^2$ (kPa) <sup>-1</sup>	$K_{\text{H}} \times 10^2$ (kPa) <sup>-0.5</sup>	$K_{\text{H}_2\text{O}}$
Reverse water gas shift						
598	$2.880 \times 10^{-3}$	2.708	0.3041	84.91	7.800	
623	$1.889 \times 10^{-2}$	3.125	0.7675	29.05	4.010	
648	$8.081 \times 10^{-2}$	3.364	1.713	9.500	1.972	
673	0.3161	3.845	3.469	4.013	1.000	
Methane steam reforming						
748	14.13		24.46			0.7158
773	41.75		45.61			0.7681
798	119.9		74.08			0.8369
823	310.8		123.0			0.9014

Afterwards, the Arrhenius and van Hoff equations were applied

$$k_i = A_i \exp\left(-\frac{E_i}{RT}\right)$$

$$K_i = A(K_i) \exp\left(-\frac{\Delta H_{i,a}}{RT}\right)$$

Table 4: Activation energies, adsorption enthalpies and other factors

	$E_1$ (kJ/mol)	$E_2$ (kJ/mol)	$E_3$ (kJ/mol)	$\Delta H_{CO,a}$ (kJ/mol)	$\Delta H_{H,a}$ (kJ/mol)	$\Delta H_{H_2O,a}$ (kJ/mol)
<i>t</i> -value	209.2 (82.4)	15.4 (8.32)	109.4 (55.0)	-140.0 (63.6)	-93.4 (25.2)	15.9 (11.4)
UL <sup>a</sup>	214.2	19.0	111.8	-135.7	-86.1	18.6
LL <sup>b</sup>	204.2	11.8	107.0	-144.3	-100.7	13.2
	$A_1$	$A_2$	$A_3$	$A(K_{CO})$	$A(K_H)$	$A(K_{H_2O})$
	$5.922 \times 10^8$	$6.028 \times 10^{-4}$	$1.093 \times 10^3$	$5.127 \times 10^{-13}$	$5.68 \times 10^{-10}$	9.251

Here are the constants being used listed. Where UL<sup>a</sup> is the upper limit and LL<sup>b</sup> is the lower limit.

The paper moves to now to its conclusion stating that at low methane conversion and low temperatures, the rate of reaction of the methane steam reforming was of the first order when referring to methane. A higher steam:methane favors more syngas production.



Finding a helpful isothermal mathematical model for a membrane reactor to further the understanding of kinetics from the *Mathematical modelling of methane steam reforming in a membrane reactor: an isothermic model* E.M. Assaf [52], C.D.F. Jesus[53] and J.M. Assaf [53]

This paper is pretty self-explanatory from its title. A one dimensional, isothermal, stationary membrane type reactor was modeled and the yield, conversion and other aspects were compared to a traditional fixed bed reactor. This proved significantly helpful as it answered many of the questions which arose during the simulation phase of the project.

First law of Fick's was used to define the diffusion of hydrogen. Temperature, flow rates, membrane thickness were all tested and the results clearly find the membrane superior to fixed bed with its higher conversion.

Nickel catalyzes the reversible reactions taking place with approach to equilibrium being achieved in the industry. However, the ATE can be shifted to higher numbers if a membrane can be used to remove hydrogen from the reactor. The fixed bed is primarily a multi-tubular packed bed reactor, the temperature of which is limited at the end of the primary reformer due to metallurgical restrictions.

The paper moves towards the mathematical modeling with the equation of a one dimensional, steady state, isothermal, pseudo-homogenous model through the following equation.

$$dX_i/dz = (\rho_b AR_i)/F_{CH_4}$$

F is the molar flow,  $X_i$  is the conversion of component  $i$ ,  $z$  is the length of the reactor,  $\rho_b$  is the density of the catalyst bed, A is the cross sectional area and  $R_i$  is the rate of reaction. The differential equations were solved using the RK-4 method.

$$R_1 = k_1^0 e^{-E_{a1}/RT} (P_{CH_4} - P_{CO} P_{H_2}^3 / Keq_1 / P_{H_2O}) / P_{TOT}^{0.5}$$

$$R_1 = k_2^0 e^{-E_{a2}/RT} (P_{CO} - P_{H_2} P_{CO_2} / Keq_2 / P_{H_2O}) / P_{TOT}^{0.5}$$

The equations above were used for the kinetic modeling with the first one being for methane steam reforming and the second for the water gas shift reaction. Here,  $R$  is the rate of the equation,  $K^{\circ}$  represents the reaction rate coefficient,  $E_a$  is the activation energy,  $T$  is the temperature,  $R$  is the gas constant,  $P$  is the pressure,  $K_{eq}$  is the equilibrium constant.

Finding palladium and silver-palladium alloys are very efficient in separating hydrogen from the rest of the gases in the mixture. They are very expensive though and have poor mechanical resistances. A metal/ceramic membrane will be an adequate balance between cost and performance.

The paper reports [31-33] as having modeled the membrane reactor and takes many of the following formulae and notions from it. An external steel shell which has either a ceramic or a metallic or a combination of the two as a porous tube inside the shell. Nitrogen is the sweep gas and methane and steam are continuously fed to the reactor in the convection zone. Itoh et al. and Shu et al. used a one dimensional, steady state isothermal and isobaric reactor [31, 33]

Fick's first law for the palladium membrane is as follows:

$$Q_H = (D_H A_m / t_m)(C_r - C_s)$$

Where  $D_H$  is the diffusivity for hydrogen,  $t_m$  is the thickness of the membrane,  $C_r$  and  $C_s$  are hydrogen concentrations and  $A_m$  is the area of the membrane calculated from the formula below.

$$A_m = \pi d_m L$$

Where  $d_m$  is the external diameter of the tubes and  $L$  is the length.

The diffusivity used was from Lewis, 1967 and was slightly modified [35].

$$D_H = 3.6 \text{ E-}5(-3.55+0.0058T)$$

Overall, the study established the material balance on the reaction side as:

$$du_i/dL = r_i A - Q_i/L$$

And on the permeation side as:

$$dv_i/dL = Q_i/L$$

$u_i$  and  $v_i$  are the fluid velocities on the permeation side and  $r_i$  the reaction rate.

The results concluded that when the membrane reactor was utilized, methane conversion was always higher. A 16% increase in yield was noted and at higher temperatures, the approach to equilibrium point was increased so more conversion took place as has already been established by convention.

Another conclusion was that the thinner the palladium film, the higher the methane conversion. This is basically because there is lesser resistance while mass transfer is taking place. However, the thinner the membrane, the more structurally compromised it became. Therefore a compromise between thinness and mechanical strength was reached with the thickness as it was supported on a ceramic base. The thickness, experimentally, ranges from  $5 \times 10^{-6}$  to  $20 \times 10^{-6}$  according to Jemaa et al [36].

Flow rate also played a part as when the initial flow of hydrogen was increased, the lesser methane conversion took place.

This paper provided valuable insight towards the trends this technology will soon be facing in the near future.

Furthering the understanding of kinetics using the paper *Methane/steam global reforming kinetics over the Ni/YSZ of planar pre-reformers for SOFC systems* by Van Nhu Nguyen et al.

The research paper investigates the kinetics to pursue a solid oxide fuel cell design on a planar stack base. The paper was based on pre-reforming rather than primary reforming however it offered valuable insight towards the kinetics to be used during the simulation of the unit.

Two types of pre reformer designs were used:

1. Five layers with air heating
2. One layer with electric heating

Both of these designs used nickel yttria-stabilized zirconia for the catalyst.

The results propose the Arrhenius kinetic reaction type-second order with respect to methane. This allowed research into how the Langmuir Hinshelwood Hougen Watson can be transformed to this form for the simulation as ASPEN Plus recognizes Arrhenius equations only under the POWERLAW reactions.

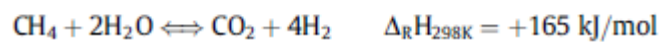
The syngas from the methane steam reforming is a requirement for SOFC systems because of the hydrogen content from syngas. Ni/YSZ is a common anode used for SOFC systems as it serves as a catalyst for the hydrogen and an anode as well. At the anode, electrochemical and reforming reactions take place at the same time. The heat required for the endothermic reforming reaction is provided by the anode heating up as the electrochemical reaction proceeds. This is known as internal reforming [37].

For external reforming, methane is reformed outside the electrochemical chamber in a pre-reformer and then the products of the process are fed to the SOFC. Pre-reforming is preferred because it stops carbon from depositing in the stack on the anode through the cracking of hydrocarbons and also avoids any inhomogeneous temperature sinks [39] because of the endothermic reforming reaction in internal reforming [37, 38]

The paper claims that a pre-reformer essentially minimizes gas-phase reactions, avoids heat losses and reduces thermal mass in order for rapid startup. [40]

The study's five layered air heated pre-reformer consisted of sub-components which provided air and held the catalyst on a wire mesh all enclosed within a solid frame.

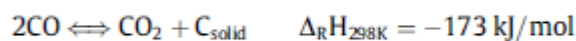
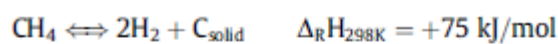
The catalyst is sandwiched between the wire mesh to increase surface area to volume ratio of the bed. The study further delves into the anode off gas recycle system and how it enhances fuel utilization. It is to be noted that the recycle system merely is for recycling unreacted methane and steam back to the pre-reformer. The efficiency which this mechanism offers to the total system is 20% higher than that of the external production of steam as this way less steam has to be generated.



Because of the endothermic reaction, 700°C or around that is used for industrial steam reforming. As more gases are produced, the volume expands which is why low pressure is used but not too low otherwise poor diffusion is resulted. A higher steam to carbon ratio favors the conversion of methane [41].

More steam will lead to more methane conversion. More steam also reduces the probability of carbon deposition, which is also dependent on the type of catalyst being used [42].

Nickel is used primarily as the catalyst for steam reforming and if the catalyst is subjected to reducing conditions, the hydrocarbons can form carbon on the surface. This can lead to active sites on the catalyst being blocked.



Methane and carbon monoxide decomposition can occur and risk carbon deposition on the surface of the catalyst. The risk can be thermodynamically quantified using [43]:

$$-\Delta G_c = \mathfrak{R} \cdot T \cdot \ln \left\{ K_{\text{eq}} \left[ \frac{P_{\text{CH}_4}}{P_{\text{H}_2}^2} \right]_{\text{equilibrated gas}} \right\}$$

If  $-\Delta G_c$  is  $>0$  then carbon will deposit on the surface of the catalyst. The research paper moves on to state that the carbon deposition limits are a function of Oxygen to

Carbon, Steam to Carbon and absolute pressure. Analyses were conducted in the study to find out the steam to carbon ratios for carbon deposition with the values of 0.88 at 812°C, 1.1 at 704 °C and 1.2 at 613°C [43]. The findings of the paper were that a steam to carbon ratio above 1.6 in the optimal temperature regions ensured very little carbon deposition [42]. Low steam to carbon ratio helps reducing the size of the reformers as well as the steam production which all helps to reduce costs. Modern reformers operate at a steam to carbon ratio of 1.8-2.5 [44].

The paper moves onwards to the kinetics and describes the kinetics in two approaches Arrhenius and Langmuir Hinshelwood. [45]

The assumption, based on literature, for the study was to consider the water gas shift reaction to be in equilibrium. This yields the following approaches for global reaction kinetics:

$$r_{\text{AAT}} = k \cdot p_{\text{CH}_4}^{\alpha} \cdot p_{\text{H}_2\text{O}}^{\beta}$$

$$k = F \cdot \exp\left(\frac{-E_a}{\mathfrak{R} \cdot T}\right)$$

However the study mentions that the reaction orders vary significantly in terms of orders of methane and water,  $\alpha$  and  $\beta$  respectively. The reaction order with respect to methane varied from 0.85 to 1.4. The reaction order with respect to water varied immensely. Achenbach and Riensche discovered it to be zero, Ahmed and Foger and Lee et al. found it to be negative, Leinfelder found it as a positive first order reaction [45,46-48].

Some revealed both negative and positive values for reaction order with respect to water [49, 50]. Small steam to carbon ratios yield a positive value whereas a large steam to carbon ratio yields a negative value. A steam to carbon ratio of 2 gives a value close to zero.

The study then goes about on the historic deviations of activation energies finally moving towards the experiment itself. The experiment involved Ni  $\pm$  8YSZ catalyst (8YSZ:8 mole% Y<sub>2</sub>O<sub>3</sub>- stabilized ZrO<sub>2</sub>) with 50% by weight Ni and 40% porosity. The flow of fuel across the surface of the catalyst were separated by the catalyst and arranged in counter flow. There were 5 layers in this arrangement and operated at 620 °C. The reactor volume was 0.336 dm<sup>3</sup>.

The second arrangement had a single plate and was electrically heated operating at 750°C. After the reforming reactions the products were analyzed using a gas chromatographer. The reactor volume was 0.067 dm<sup>3</sup>. The next step was to activate the catalyst using reducing agents like hydrogen gas.

The results showed that the conversion of methane

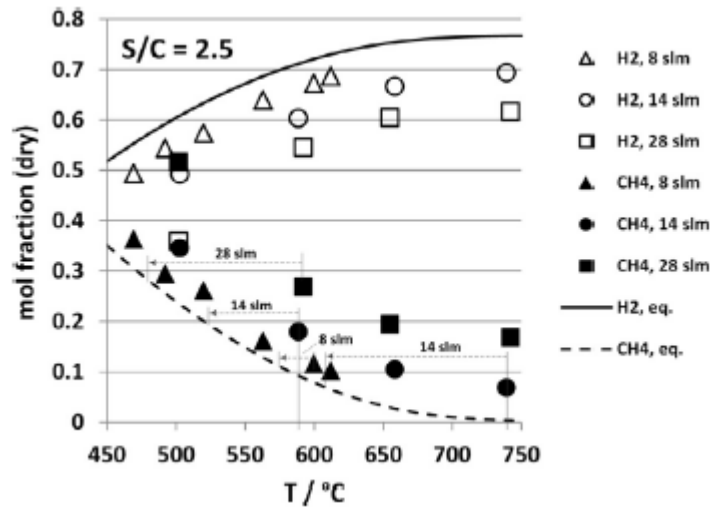


Figure 3: Exemplary product compositions of dry gaseous species Hydrogen and Methane at different volumetric flow rates as a function of S/C=2.5

The temperature difference  $\Delta T_d$  shows the approach to equilibrium. For more space time, ATE is closer to zero. Ultimately, the results showed that methane conversion increases with increasing space time [51] and increasing steam to carbon ratio.

For the kinetics part, the paper concluded that the rate determining step or the slowest rate step is the absorption of methane on the catalyst's surface.

$$\begin{aligned} r_{r,Arr} = -r_{CH_4} &= -\frac{d(x_{CH_4})}{d\tau} = -\frac{d(x_{0,CH_4} - \xi)}{d\tau} = \frac{d(\xi)}{d\tau} \\ &= k \cdot (x_{0,CH_4} - \xi)^2 \cdot (x_{0,H_2O} - \xi) \end{aligned}$$

Where  $\xi$  is the value of the progress, determined by how large is the ATE, of the reforming reaction.

The conclusions presented by the study reveal a corrected value for activation energy for the reactions occurring in a 5 layered reformer, methane conversion and its dependency on factors, the proposed kinetic model of Arrhenius type (second order when referring to methane and first order when considering steam), Activation

energy of  $62 \pm 5 \text{ kJ mol}^{-1}$  for methane steam reforming with no carbon monoxide at the inlet.



# Chapter-3

## Methodology

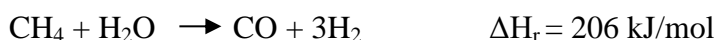
The approach for dealing with this project involves firstly balancing the mass and energy and then moving on towards the reaction kinetics. Once this was done the approach proceeded towards the modeling aspects leading to simulation. Simulating on Aspen Plus provided with greater freedom to mimic close to realistic conditions.

First and foremost was the material balance which was begun after research into the methodology and meetings with the industrial supervisor. Using the approach to equilibrium methodology it was established the extent of reactions and then rechecked them with the provided information of the industry. The errors faced were primarily due to the insistence of the industrial supervisor for neglecting the reactions of ethane in the reformer.

### 3.1. Material Balance:

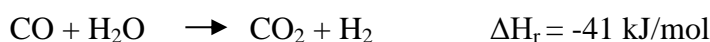
As has been discussed previously in the process description, methane steam reforming and the water gas shift reaction take place in the reformer. They take place in the convection zone of the reformer.

The main reaction is the reforming one, which is stated as follows:



The above reaction is endothermic, the heat of which is provided partially by the water gas shift reaction and the remainder by the furnace installed where methane gas is combusted.

The following reaction is the water gas shift reaction.



As far as the combustion reaction taking place in the furnace are concerned, methane is largely the fuel used with negligible amounts of ethane undergoing combustion which was ignored due to insistence of the supervisor.



The exhaust flue gases which result from the combustion inside the furnace exit through the chimney after exchanging their energy with incoming feed streams to recover the heat. The following block flow diagram represents the streams entering and leaving the reformer.

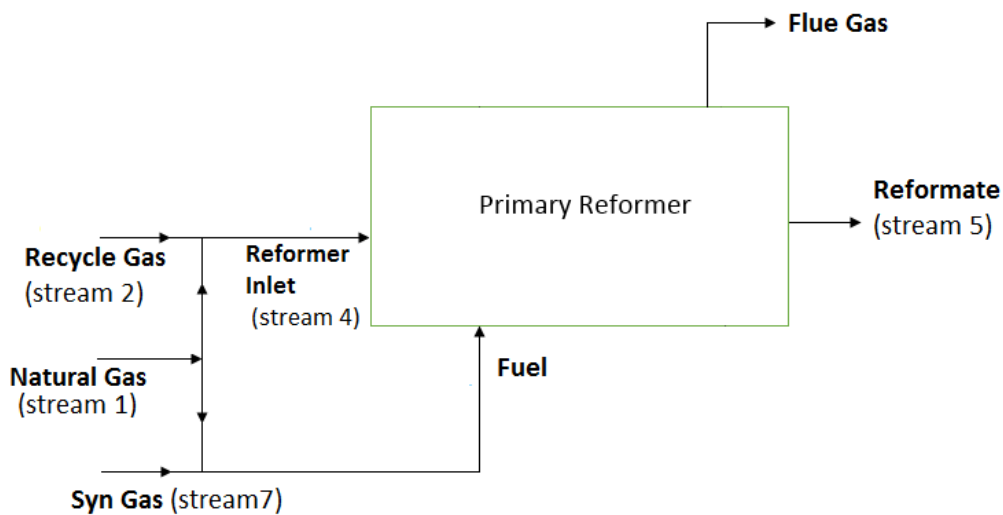


Figure 4: Block diagram for balances

Because the flow rates were provided in  $\text{Nm}^3/\text{h}$ , the temperature and pressure of all the streams were taken as 273.15 K and 101.325 kPa respectively.

The use of  $\text{Nm}^3/\text{h}$  made the procedure extremely easy as there was no deviation from the ideal gas equations for the calculation of the remaining quantities. The next step was to use the molecular masses of the gaseous compounds to determine the densities of the streams. For this, the Ideal gas equation was used:

$$PV=nRT$$

Where n is the number of moles, P is the pressure, V is the volume, R is the gas constant and T is the temperature. The members expanded it to the form:

$$PV = (\text{mass}/M_r)RT$$

Where  $M_r$  is the molecular mass. The members then rearranged the equation to:

$$\rho = (P)(M_r)/RT$$

Where  $\rho$  is the density of the gas in  $\text{kg}/\text{m}^3$ . The value of  $R$  was equal to  $8.314 \text{ J mol}^{-1} \text{ K}^{-1}$

Now, density was available alongside the volumetric flow rate could easily determine the mass flow rate.

$$\text{Mass flow rate} = (\text{volumetric flow rate}) (\text{density})$$

The mass flow rates were incredibly important as they were the only way to realize mass conservation along the reactor. Converting mass flow rates to molar flow rates was also crucial for the stoichiometric balances which were used to cross check.

Finally, the molar composition of the components was determined which was cross checked with the molar/volumetric composition provided to by the industry.

The following table represent the components of the inlet stream which was calculated using the 3 streams initially provided the information of.

Table 5: Inlet stream to reformer

<b>Compound</b>	<b>Kg/Kmol</b>	<b>Kg/m<sup>3</sup></b>	<b>Nm<sup>3</sup>/h</b>	<b>Kmol/h</b>	<b>Kmol/Kmol</b>
<b>Nitrogen</b>	28.01	1.250	7720	344.45	0.0631
<b>Hydrogen</b>	2.01	0.090	1791	79.91	0.0146
<b>Carbon Dioxide</b>	44.01	1.964	3138	140.01	0.0256
<b>Argon</b>	39.95	1.782	6	0.27	4.9x10 <sup>-5</sup>
<b>Methane</b>	16.04	0.716	28990	1293.46	0.2370
<b>Water</b>	18.05	0.805	80713	3601.21	0.6596
			<b>122358</b>	<b>5459.31</b>	<b>1</b>

Information about the other streams 1 (natural gas from Mari), 2 (recycle gas) and 7 (syngas) were provided attached here:

Table 6: Stream compositions and parameters

Stream	Compound	Nm <sup>3</sup> /h	kmol/h	kmol/kmol
<b>1</b> <b>Natural</b> <b>Gas</b>	<b>Nitrogen</b>	10151	452.912	0.180
	<b>Carbon Dioxide</b>	4511	201.267	0.080
	<b>Methane</b>	41617	1856.847	0.739
		<b>56279</b>	<b>2511.029</b>	<b>1</b>
<b>2</b> <b>Recycle</b> <b>Gas</b>	<b>Hydrogen</b>	1791	79.910	0.717
	<b>Nitrogen</b>	659	29.403	0.264
	<b>Argon</b>	6	0.268	0.002
	<b>Methane</b>	39	1.740	0.016
	<b>Water</b>	4	0.1785	0.002
		<b>2499</b>	<b>111.499</b>	<b>1</b>
<b>7</b> <b>Syngas</b> <b>Fuel</b>	<b>Hydrogen</b>	1050	46.848	0.716
	<b>Nitrogen</b>	386	17.222	0.263
	<b>Argon</b>	4	0.1785	0.003
	<b>Methane</b>	23	1.026	0.016
	<b>Water</b>	4	0.178	0.003
		<b>1467</b>	<b>65.454</b>	<b>1</b>

From these the inlet stream was calculated to the furnace and the inlet to the reformer (shown above) through simple arithmetic and the principle of conservation of mass.

The calculations were performed after the inlet to the reformer was determined. The material balance was applied across the reformer. The approach to equilibrium method was used to determine the amount of conversion the two reactions underwent. The first reaction's conversion was assumed initially and using that, the concentration of methane in the exit stream was determined. Then used the exit temperature of the stream to find out the equilibrium constant  $K_p$  and used the formula  $K_p = \frac{(CO)(H_2)^3}{(CH_4)(H_2O)}$ . Establishing the values for the methane steam reforming, the same principle to water gas shift reaction with the formula for  $K_p = \frac{(CO_2)(H_2)}{(CO)(H_2O)}$  was applied.

Having two values of conversions, one for each reaction, and two values of  $K_p$  the actual values for  $K_p$  from the literature were compared with. Then goal seek was used to change the values of  $K_p$  to achieve the desired conversion. What this helped do was provide the partial pressures for each reaction. This was rechecked with the calculations below and found to be correct.



Steam here is in excess as the steam to methane ratio provided is 2.8:1 which was determined by simply dividing the molar flow rates of the two components.

Using ATE, it was established that the conversion of the methane steam reforming reaction to be 60.03% which provided the extent of the reaction on basis of methane =  $1293.46 - 517.03 = 776.43$  kmol/h

776.43 kmol/h of methane will produce:

$$3 \times 776.43 = 2329.30 \text{ kmol/h of Hydrogen}$$

$$1 \times 776.43 = 776.43 \text{ kmol/h of Carbon Monoxide}$$



ATE also provided with the conversion of the water gas shift reaction, which was 38.86% which translated to an extent of the reaction on basis of Carbon monoxide =  $776.43 - 474.69 = 301.75$  kmol/h

301.75 kmol/h will produce:

1 x 301.75 kmol/h= 301.75 kmol/h of CO<sub>2</sub>

1 x 301.75kmol/h= 301.75 kmol/h of H<sub>2</sub>

Total H<sub>2</sub> in the outlet = 301.75 + 2329.30 = 2631.05 kmol/h

Total CO<sub>2</sub> in the outlet = 140.01 + 301.75 = 441.76 kmol/h

Water in the outlet = 3601.21 - 776.43 - 301.75 = 2523.03 kmol/h

The Following Table represents the reformer material balance:

Table 7: Reformer material balance

<b>Reformer Material Balance</b>			
<b>Compound</b>	<b>Moles in (kmol/h)</b>	<b>Moles Out (kmol/h)</b>	<b>Moles Reacted/Formatted</b>
<b>Methane</b>	1293.46	517.03	-776.43
<b>Water</b>	3601.21	2523.03	-1078.18
<b>Carbon monoxide</b>	0	474.69	-301.75
<b>Carbon dioxide</b>	140.01	441.76	301.75
<b>Hydrogen</b>	79.91	2631.05	2551.14
<b>Nitrogen</b>	344.45	344.45	0
<b>Argon</b>	0.27	0.27	0

### **3.2. Energy Balance:**

Following are the heats of two reactions:

Heat of Methane Reforming Reaction =  $2.06 \times 10^5$  kJ/kmol

Heat of Methane Reforming Reaction =  $1.6 \times 10^8$  kJ/h

Heat of Water Gas Shift Reaction =  $-4.1 \times 10^4$  kJ/kmol

Heat of Water Gas Shift Reaction =  $-1.237 \times 10^7$  kJ/h

The first step was to determine the temperature of the fuel entering the furnace of the reformer. Two streams, natural gas and syngas mix together and proceed into the burner area.



### 3.2.1. Fuel Mixing Point:

Table 8: Fuel mixing point

<b>Fuel Mixing point</b>			
<b>Stream</b>	<b>Component</b>	<b>Molar Flow Rate kmol/h</b>	<b>Temperature K</b>
<b>Syngas</b>	<b>Hydrogen</b>	46.85	311.15
	<b>Nitrogen</b>	17.22	311.15
	<b>Argon</b>	0.18	311.15
	<b>Methane</b>	1.03	311.15
	<b>Water</b>	0.179	311.15
<b>Natural Gas</b>	<b>Nitrogen</b>	452.91	308.15
	<b>Carbon Dioxide</b>	201.27	308.15
	<b>Methane</b>	1856.85	308.15
<b>To Burners</b>	<b>Hydrogen</b>	46.85	308.21
	<b>Nitrogen</b>	470.14	308.21
	<b>Argon</b>	0.18	308.21
	<b>Methane</b>	1857.87	308.21
	<b>Water</b>	0.18	308.21
	<b>Carbon Dioxide</b>	201.27	308.21

Temperature of Natural gas at mixing point = 35 °C

Temperature of Syngas at mixing point = 38 °C

Fuel mixing point is a point where the Natural gas and Syngas combine to give the resultant stream which goes to the burner as its feed.

The Temperature of the components of “To Burner” Stream was found out by

$$\frac{(\text{Molar flow of each component of both streams}) \times (\text{Heat capacity of each component}) \times (\text{respective } \Delta T)}{(\text{Molar flow of each component of both streams}) \times (\text{Heat capacity of each component})}$$

The temperature of the resultant stream came out to be 35.06 °C or 308.21 K

The energy data of the components at 35 °C and 38 °C was taken from Perry's Handbook and rechecked by Aspen Hysys.

### 3.2.2. Burner Balance:

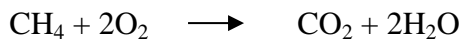
Inlet Temperature to burners = 35.06 °C

Outlet Temperature to burners = 1015 °C

Heat of Reaction in Burner =  $-8.9 \times 10^5$  kJ/kmol or  $-4.61 \times 10^8$  kJ/h

Using the tool of Goal seek in Excel, the known value of Burner duty was approached by altering the conversion.

Following reaction takes place in burner:



Assuming oxygen is in excess,

Extent of reaction on the basis of Methane =  $1857.87 \times 0.28 = 517.24$  kmol/h

1857.87 moles of methane will require =

$2 \times 1857.87 = 3715.75$  kmol/h

Methane in the product =  $1857.87 \times 0.28 = 517.24$  kmol/ h

Water in the product =  $0.18 + 2 \times 1857.88$  kmol/ h

CO<sub>2</sub> in the product =  $201.27 + 1 \times 1857.87 = 718.51$  kmol/ h

O<sub>2</sub> in the product =  $3715.75 - 2 \times 517.24 = 2681.27$  kmol/ h

Using the data of moles and the data of Heat capacity and Standard heat of formation at Inlet and outlet temperatures, Molar Enthalpies and Energies were calculated by following formulae:

$$\Delta H = H_f + C_p \Delta T$$

$$\Delta E = m \times \Delta H$$

The energy data of the components at 35 °C and 38 °C was taken from---

Following table shows the burner energy balance across the furnace.

Table 9: Furnace balance

<b>Compound Type</b>	<b>Moles In (kmol/h)</b>	<b>Energy In (kJ/h)</b>	<b>Moles Out (kmol/h)</b>	<b>Energy Out (kJ/h)</b>
<b>Hydrogen</b>	46.85	1.34x10 <sup>4</sup>	46.85	1.46x10 <sup>6</sup>
<b>Nitrogen</b>	470.14	1.43x10 <sup>5</sup>	470.14	1.57x10 <sup>7</sup>
<b>Argon</b>	0.18	39.58	0.18	3.7x10 <sup>3</sup>
<b>Methane</b>	1857.87	-1.38x10 <sup>8</sup>	51.78	2.91x10 <sup>5</sup>
<b>Water</b>	0.18	-4.3x10 <sup>4</sup>	3612.37	-7.14x10 <sup>8</sup>
<b>Carbon Monoxide</b>	0	0	0	0
<b>Carbon Dioxide</b>	201.27	-7.91x10 <sup>7</sup>	2007.36	-6.76x10 <sup>8</sup>
<b>Oxygen</b>	3715.75	1.14x10 <sup>6</sup>	103.56	3.7x10 <sup>6</sup>
<b>Sum</b>	<b>6292.23</b>	<b>-2.16x10<sup>8</sup></b>	<b>6292.23</b>	<b>-2.98x10<sup>9</sup></b>

### 3.2.3. Reformer Energy Balance:

The inlet feed stream enters the reformers at 600 °C and the outlet stream leave at 808 °C. Moles of these streams entering and leaving the reformer were calculated in the material balance part. Using that and the data of Heat capacity and Standard heat of formation at different temperatures, Molar Enthalpies and Energies were calculated by following formulae:

$$\Delta H = H_f + C_p \Delta T$$

$$\Delta E = m \times \Delta H$$

Ultimately, the heat duty for the reformer was calculated to be 35Gcal/h (146,440,000 kJ/h) which was achieved using a 97.213 % conversion of methane to its combustion products.

### 3.2.4. Summarized Energy Balance:

Heat in to reformer = Sum of the energy of all components of Inlet feed stream entering the reformer

Heat out of reformer = Sum of the energy of all components of Inlet feed stream leaving the reformer

Heat into burner = Sum of the energy of all components of fuel entering the burner

Heat out of burner = Sum of the energy of all components of fuel leaving the burner

Heat consumed by reaction 1 = Extent of reaction x heat of reaction

Heat consumed by reaction 2 = Extent of reaction x heat of reaction

Heat released by combustion in burner = Extent of reaction x heat of reaction

Heat duty = Heat of reaction 1-Heat of reaction 2+ Waste heat

Waste heat includes Energy out of reformer + Energy out of furnace.

### **3.3. Simulation:**

In order to model and consolidate the project, the members modeled the project using ASPEN Plus. ASPEN Plus was used instead of HYSYS because of the variety of options it offers in selection of reactor and its kinetics. The primary reformer, which is basically a tubular plug flow reactor, is simulated near to its conditions on ASPEN Plus.

Peng Robinson fluid package was used as it deals in close to real results for gases. The degree of uncertainty it offers is far less than the other models like SRK or NRTL.

The desulfurization tank is also added as it is an important part of the project. As there is no sulfur in the feed, the vessel barely comes into operation but it acts as a fail-safe in case there are traces of sulphur in the feed which can de-activate the catalyst.

A furnace is added in the simulation. In the Process Flow Diagram, no separate furnace is shown as it is a part of the primary reforming section in the plant. However, the reformer is basically two sections, a convective section and a radiant one with the latter being the furnace which provides energy to the convective section in which endothermic reactions take place. There are burners in the furnace and the entire unit is naturally aspirated or self-aspirated. Fuel is combusted and the heat of the combustion reaction is transferred in the furnace. Hence it becomes important to include the furnace in the simulation separately as an entity. One of the primary reasons to incorporate it as a separate unit was to basically modularize the simulation which made adjustments later on in the stage quite easy.

Next on, two fail safe valves are also added into the feed stream of the reformer. The valves acts as fail close valve. This is because in case of a no-response in signal, the valve will close and stop the gases from flowing into reformer and from reaction to proceeding and raising heat

The furnace which has all burner acts as the radiation section of the Primary reformer. Fuel is burnt and heat radiated to help speed up the endothermic reaction. The radiation section has four burners all aligned together. The fuel for the burners is

methane gas basically or the natural gas brought in from Mari. It is used as a raw material in the convection section as well as a fuel source in the radiation section.

Before any simulation, the members have to establish a model. The material and energy balances proved very helpful in examining the validity of the model once the members established it. The credit for the model goes to Kaihu Hou, et al. for providing an extremely detailed account of the Langmuir Hinshelwood Hougen Watson kinetic model, elaborated on in the literature review, to simulate.

The first step was to start with a blank simulation, there are templates installed for other practices as well but the blank simulation gave the freedom to explore opportunities within the software.

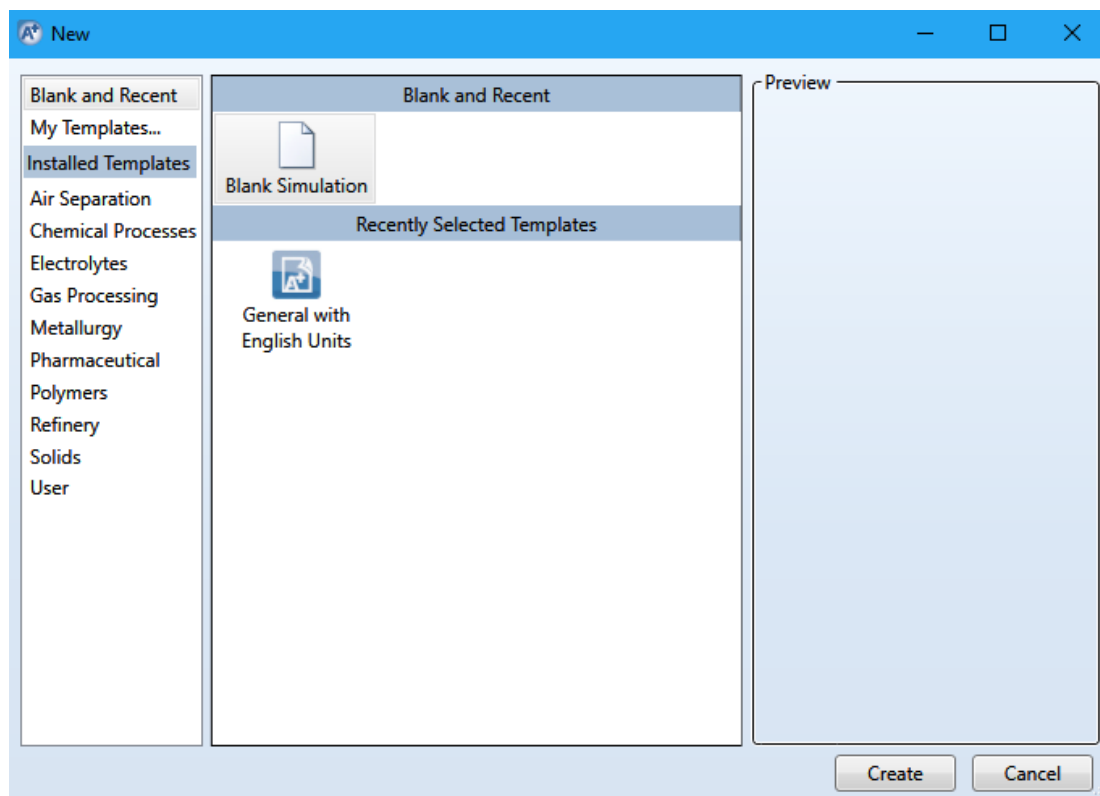


Figure 5: Initiation step for simulation

The second step involved adding the components which are listed in the following image, please note that the names can be changed by changing the component ID and have been in some cases. This allowed easily move through the complexities which were to follow.

Select components:

Component ID	Type	Component name	Alias
AMMONIA	Conventional	AMMONIA	H3N
NITROGEN	Conventional	NITROGEN	N2
HYDROGEN	Conventional	HYDROGEN	H2
METHANE	Conventional	METHANE	CH4
ETHANE	Conventional	ETHANE	C2H6
OXYGEN	Conventional	OXYGEN	O2
CO	Conventional	CARBON-MONOXIDE	CO
CO2	Conventional	CARBON-DIOXIDE	CO2
STEAM	Conventional	WATER	H2O
ARGON	Conventional	ARGON	AR

Figure 6: List of components

The next step involved selecting the property methods and setting the options. Peng Robinson was chosen as it provides with the least amount of error associated with gaseous phases of which all the components were.

Figure 7: Property method selection

Afterwards, ASPEN provided us with a number of decisions of which the members selected property analysis which checked out without any errors and moved forward with the simulation environment which is the last option in the image.

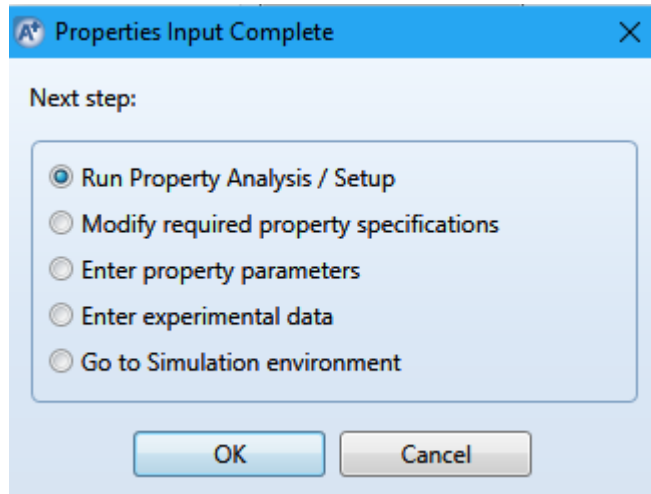


Figure 8: Properties input complete

In the simulation environment the primary focus was towards the plug flow reactor as that is essentially what is used in the industry in a more multi-tubular sense, however both the versions of ASPEN Plus v 8.4 and 8.8 stopped working as soon as the members entered the time for convergence. This forced the hand to look for alternatives and through the research onto which would prove the most accurate substitute, the members employed a Gibbs free reactor.

This compounded the difficulty of the simulation as with a plug flow reactor the members only had to provide the kinetics and the catalyst weight and voidage for the reactor to yield results which it failed to do so because of an error in its execution file during the convergence. For the Gibbs reactor, kinetics were modelled therefore on the Langmuir Hinshelwood Hougen Watson without the information of the catalyst. Luckily, the diligence during the balancing phases proved useful as the members used the methodology the members adopted with approach to equilibrium and found out during the study of the software that if the members were to provide the kinetics alongside the extent of the reaction, the approach would be automatically calculated and would yield accurate results. The members therefore adopted this approach.



The next step was to define the reactions of both the reforming section and the furnace itself. POWERLAW elaborated in the image below.

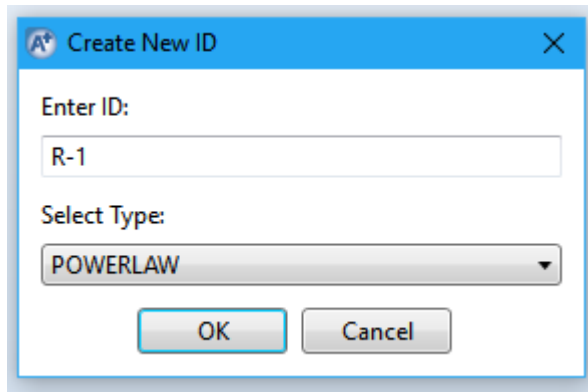


Figure 9: Reaction definition

Following the type selection, the two reforming reactions were defined and are shown below:

Rxn No.	Reaction type	Stoichiometry
1	Kinetic	METHANE(MIXED) + STEAM(MIXED) --> CO(MIXED) + 3 HYDROGEN(MIXED)
2	Kinetic	CO(MIXED) + STEAM(MIXED) --> CO2(MIXED) + HYDROGEN(MIXED)

Figure 10: Reactions properly defined

The members edited the reaction types and established the stoichiometric coefficients in the following steps an example of which is given below in the attached image.

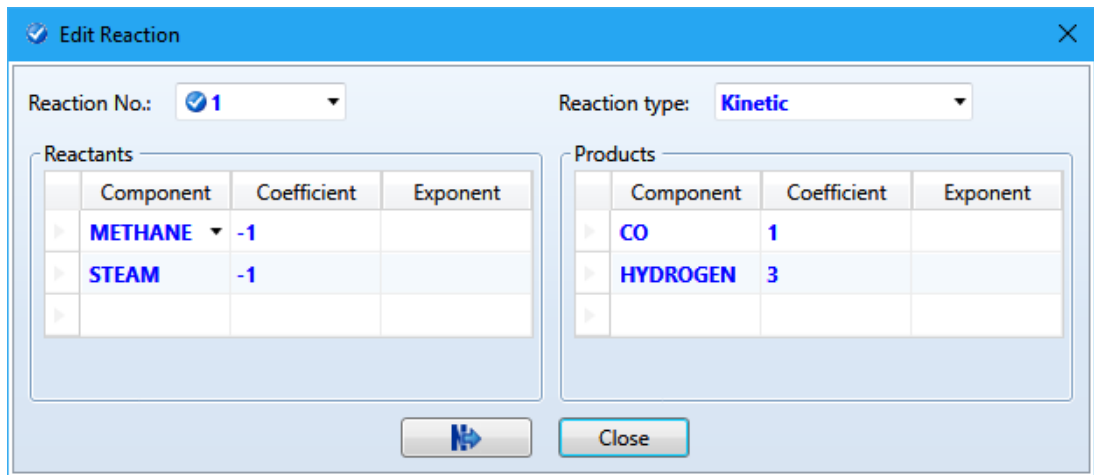


Figure 11: Stoichiometric coefficients for SMR

Once this was done the members moved on to describing the kinetics of the reactions.

1) METHANE(MIXED) + STEAM(MIXED) --> CO(MIXED) + 3 HYDROGEN(MIXED)

Reacting phase: **Vapor** Rate basis: **Reac (vol)**

Power Law kinetic expression

If To is specified: Kinetic factor =  $k(T/T_0)^n e^{-(E/R)[1/T-1/T_0]}$   
 If To is not specified: Kinetic factor =  $kT^n e^{-E/RT}$

k: **5.922e+08**  
 n: **1**  
 E: **209.2** **kJ/mol**  
 To: **K**  
 [Ci] basis: **Molarity**

Edit Reactions  
Solids

Figure 12: Kinetics for SMR

2) CO(MIXED) + STEAM(MIXED) --> CO2(MIXED) + HYDROGEN(MIXED)

Reacting phase: **Vapor** Rate basis: **Reac (vol)**

Power Law kinetic expression

If To is specified: Kinetic factor =  $k(T/T_0)^n e^{-(E/R)[1/T-1/T_0]}$   
 If To is not specified: Kinetic factor =  $kT^n e^{-E/RT}$

k: **0.0006028**  
 n: **1**  
 E: **15.4** **kJ/mol**  
 To: **K**  
 [Ci] basis: **Molarity**

Edit Reactions  
Solids

Figure 13: Kinetics for WGS

The members now had reaction set 1 complete. These reactions are to take place in the reformer and are the steam methane reforming and the water gas shift reaction. The members next moved on to making the flowsheet of the reactor which was segmented into the convective and the radiant sections. The members will now discuss the convective section where the steam methane reforming and water gas shift reactions take place:

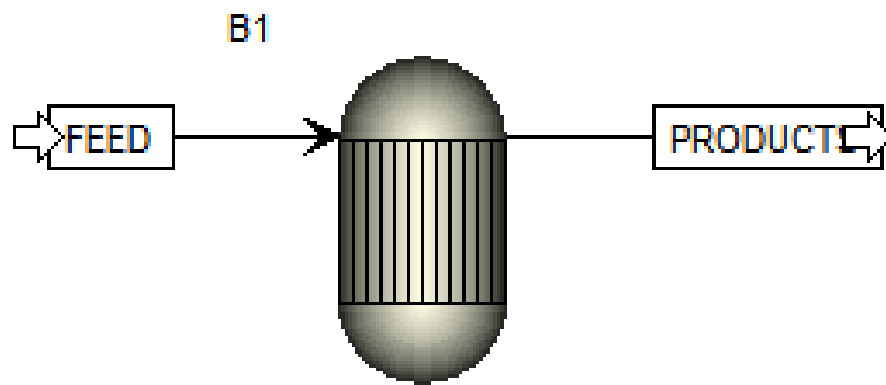


Figure 14: Reformer flowsheet

The following specifications were selected for the reactor, pressure and heat duty were added. Pressure was provided in the process flow diagram from the industry and the heat duty was calculated accurately, when compared to actual heat duty, of the reformer.

Specifications   
 Products   
Assign Streams   
Inerts   
 Restricted Equilibrium   
Utility   
Ir

Calculation option:  
**Restrict chemical equilibrium - specify temperature approach or reactions**

Operating conditions

Pressure:

Temperature:

Heat Duty:

Phases

Maximum number of fluid phases:

Maximum number of solid solution phases:

Include vapor phase

Merge all CISOLID species into the first CISOLID substream

Figure 15: Reaction specifications

The next step was crucial because otherwise this the reactor was not converging. There was a need to define the products to be expected in the outlet stream as ASPEN is open to possibilities of defining new reactions which is why there is the requirement for products to be specified.

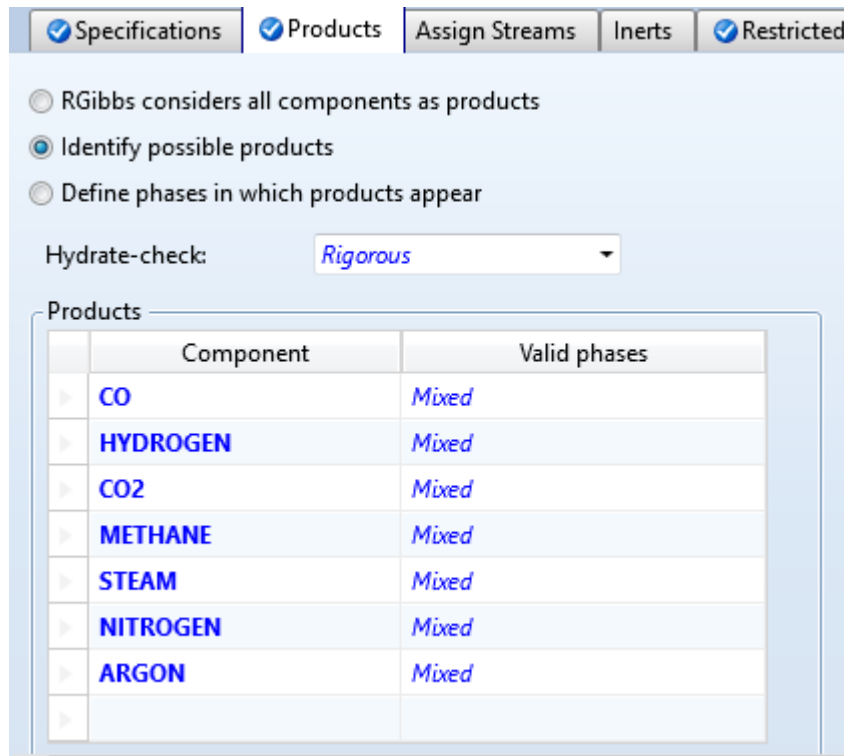


Figure 16: Possible reactants.

The members then make the necessary changes for informing the software on the approach to equilibrium.

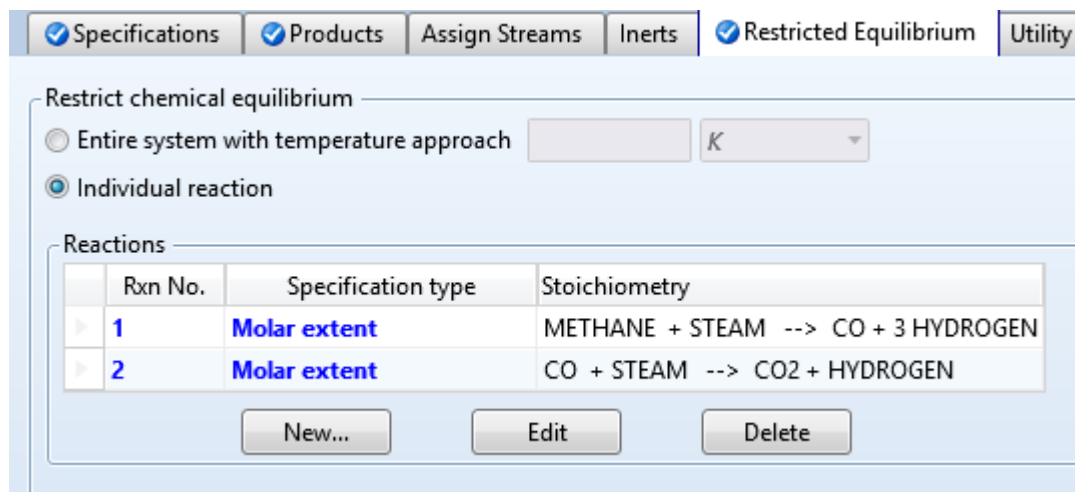


Figure 17: Molar extents defined

Once achieved, the reactor will converge. This however is the convective section only. For the furnace another reactor with the exact negative heat duty of the convective section is used to make sure the conversion of methane during combustion is a value which has a direct cause and effect with the heat released.

For the furnace the members used another Gibbs reactor because of the reasoning that the energy required is only extracted from the energy available.

Once the members added the reactor, the members followed the same procedure explained above to achieve the readings.

The image shows a software interface with several tabs: Specifications, Products, Assign Streams, Inerts, Restricted Equilibrium, and Utility. The 'Specifications' tab is active. Below the tabs, there is a 'Calculation option:' dropdown menu set to 'Calculate phase equilibrium and chemical equilibrium'. Underneath, there is a section for 'Operating conditions' with three radio buttons: 'Pressure:', 'Temperature:', and 'Heat Duty:'. The 'Heat Duty:' option is selected. The 'Heat Duty:' field has a value of '-35' and a unit dropdown set to 'Gcal/hr'. Below this is a 'Phases' section with two spinners: 'Maximum number of fluid phases:' and 'Maximum number of solid solution phases:'. The 'Maximum number of solid solution phases:' spinner is set to '0'. There are two checkboxes: 'Include vapor phase' (checked) and 'Merge all CISOLID species into the first CISOLID substream' (unchecked).

Figure 18: Specifications for WGS

After defining the products, the heat duty and following the remainder of the steps the reactor converged as well. The flowsheet now manifested into this form:

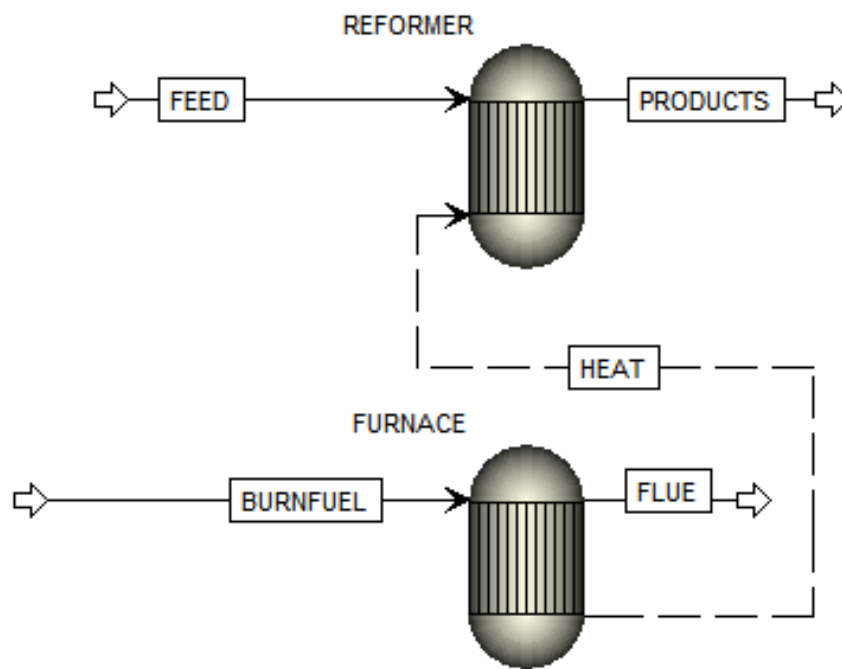


Figure 19: Flowsheet with reformer and furnace

Finally, the members added control valves on the inlets of both the sections of the reformer. The valves have complicated control loop systems which the members weren't able to recreate in the simulation.

Reconnecting the process streams by setting their destination to the start of the valves, the members ended up with the following flowsheet:

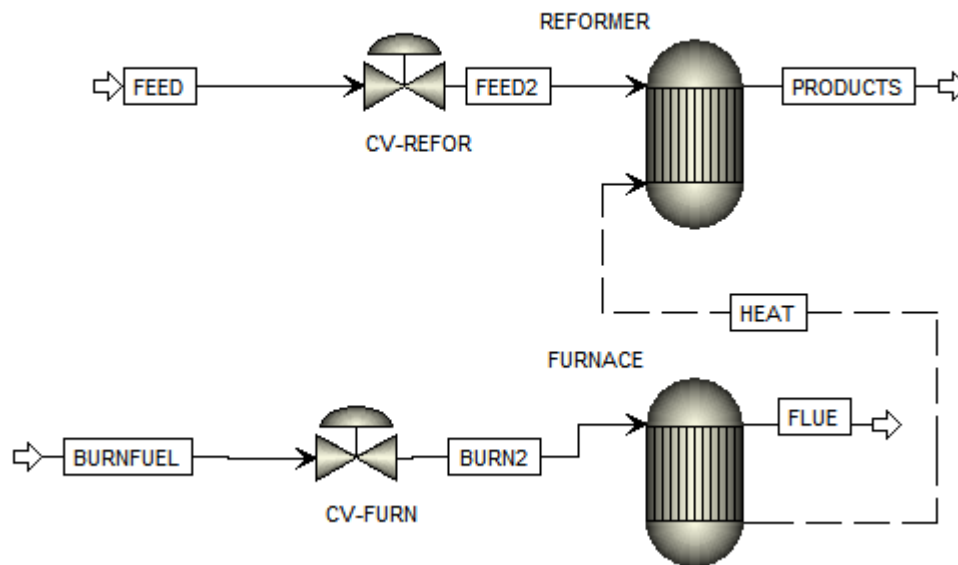


Figure 20: Overall flowsheet

Both valves were assumed to be globe valves which seemed logical as the actuators designed are not simply for opening or closing but also for varying the size of the opening. It is safe to say that most of the information was assumed while considering the simulation of the valves. They were modeled using the pre-existing equal percentage Neles-Jamesbury valves sized at 4 inches diameter.

### 3.4. HAZOP analysis

Steps which the members took for HAZOP were as follows:

1. Modularize the reformer into two sections with reforming separate from the furnace
2. Select the region for analyzing
3. Select the parameter
4. Choose guide word
5. Select deviation from standard
6. Think of possible causes
7. Find the possible consequences



The result is as follows

Table 10: HAZOP analysis of furnace

	<b>Guide Word</b>	<b>Parameter</b>	<b>Deviation</b>	<b>Cause</b>	<b>Consequences</b>
<b>1</b>	No	Temperature	No temperature	No fuel going in furnace	No combustion
<b>2</b>	Low	Temperature	Low temperature	Improper supply of fuel	Incomplete combustion
<b>3</b>	High	Temperature	High temperature	Higher supply of fuel	Fuel loss, Equipment damage

Table 11: HAZOP analysis of reformer

	<b>Guide Word</b>	<b>Parameter</b>	<b>Deviation</b>	<b>Cause</b>	<b>Consequences</b>
<b>1</b>	No	Flow	No flow	No feed going to reformer	No reaction
<b>2</b>	Low	Flow	Low flow	Lesser supply of feed	Incomplete reaction, Loss of energy
<b>3</b>	High	Flow	High flow	Higher supply of feed	High methane and steam slippage

### 3.5. Costing:

For Costing of Primary Methane steam reformer, data of small scale Steam Methane Reforming (SMR) was taken from a report of NREL, U.S. Department of Energy Office of Energy Office of Energy Efficiency & Renewable Energy. Extrapolation methodology was used to calculate cost of equipment in the project.

#### 3.5.1. Reactor Cost:

Data of Primary Methane steam reformer in the project:

$$\text{Reactor volume} = 25 \text{ m}^3$$

$$\text{Reactor length} = 10.5 \text{ m}$$

$$\text{Reactor radius} = \sqrt{V/\pi h} = 0.87 \text{ m} \quad \text{Reactor Diameter} = 0.87 \times 2 = 1.741 \text{ m}$$

Number of tubes 180

$$\text{Length of each tube} = 10.5 \text{ m}$$

$$\text{Inner diameter} = 138 \text{ mm} \quad \text{Outer diameter} = 152 \text{ mm}$$

According to the data given in the costing source, following are the specification of Reformer bed

Shell:

$$\text{Length} = 40 \text{ inch} = 1.016 \text{ m}$$

$$\text{Diameter} = 14 \text{ inch} = 0.3556 \text{ m} \quad \text{radius} = d/2 = 0.1778 \text{ m}$$

$$\text{Volume of shell} = \pi r^2 h = 0.1009 \text{ m}^3$$

Tube:

$$\text{Length} = 39 \text{ inch} = 0.9906 \text{ m} \quad \text{Diameter} = 0.5 \text{ inch} = 0.0127 \text{ m}$$

Materials = Incoloy 800H (shell) & Haynes 556 (Tubes)

$$\text{Cost of reactor} = \$28,746$$

Using Extrapolation technique

$$\text{Cost of } 0.1009 \text{ m}^3 \text{ volume reactor} = \$28,746$$

Cost of  $25\text{m}^3$  volume reactor = \$7122400

### 3.5.2. Cost of Hydrogen-Desulphurization Tank:

According to the data given in the costing source, following are the specification of Hydro-Desulphurization Tank (HDS):

Diameter = 4inch = 0.1016m

Length = 30inch = 0.762m

Volume of shell =  $\pi r^2 h = 0.006174\text{m}^3$

Cost of HDS tank = \$5,277

Material Used: 316SS

Using Extrapolation:

When length of reactor shell in the source is 40 inch then actual length = 10.5m

So when length of HDS tank in the source is 30 inch then actual length =  $(10.5/40) \times 30 = 7.875\text{m}$

Also,

When Diameter of reactor shell in the source is 14 inch then actual Diameter = 1.741m

So when Diameter of HDS tank in the source is 4 inch then actual Diameter =  $(1.741/14) \times 4 = 0.497\text{m}$

Radius =  $0.497/2 = 0.2485\text{m}$

Volume of Actual HDS tank =  $\pi r^2 h = 1.527 \text{m}^3$

Cost of  $0.006174\text{m}^3$  volume reactor = \$5,277

Cost of  $1.527\text{m}^3$  volume reactor = \$13,05,150

### 3.5.3. Heat Exchanger Costing:

According to the data given in the costing source:

The combined cost of Reactor and HDS tank =  $\$28,746 + \$5,277 = \$34,023$

Cost of heat exchanger used with the above setup =  $\$18,415$

But, the combined cost of Reactor and HDS tank in the project =  $\$7122400 + \$13,05,150 = \$84,27,550$

Again using extrapolation,

When combined cost in the source is  $\$34,023$  then cost of heat exchanger =  $\$18,415$

When combined cost in the project is  $\$84,27,550$  then cost of heat exchanger =  $(18415/34023) \times 8427550 = \$4561425$

Physical Cost of Equipment (PCE) =  $\$7122400 + \$13,05,150 + \$4561425 = \$1,29,88,975$

Adding all the Lang factors the members get = 2.15

Total physical Plant cost (PPC) = PCE x (1+sum of all lang factors)  
=  $\$1,29,88,975 \times (1+2.15) = \$40915280$

Sum of remaining lang factors = 0.4

Fixed Capital = PPC x (1+sum of remaining lang factors)  
=  $\$40915280 \times (1+0.4) = \$57281392$

### 3.5.4. Raw Material Cost:

According to a report [54], Natural gas is provided to FFC, Mirpur Mathelo at the following rate=

Rs.200/MMBTU for gas used as feed stock

Converting it into  $\$/\text{Nm}^3 = 200 \times (1/27.1) \times (1/100) = \$0.074/\text{Nm}^3$

Where MMBTU=  $27.1\text{Nm}^3$  and 1 \$ = Rs.100

As mentioned in the material balance, the volumetric rate of required feed is  $56279 \text{Nm}^3/\text{hr}$ . So the cost of required natural gas becomes=

$(\$0.074/\text{Nm}^3) \times (56279 \text{Nm}^3/\text{hr}) = \$4165/\text{hr}$  or  $\$29,98,800/\text{month}$

This natural gas acts as a feed stock for fuel to burners and for production of steam as well. Some amount of steam is produced by the flue gases as well.

Syngas is produced by the industry itself, so the cost for that is not considered.

So total raw material cost =  $\$29,98,800/\text{month}$

### Variable Cost and Fixed Cost:

Table 12: Variable and fixed costs methodology

<i>Variable costs</i>	<i>Typical values</i>
1. Raw materials	from flow-sheets
2. Miscellaneous materials	10 per cent of item (5)
3. Utilities	from flow-sheet
4. Shipping and packaging	usually negligible
Sub-total A	.....
<i>Fixed costs</i>	
5. Maintenance	5–10 per cent of fixed capital
6. Operating labour	from manning estimates
7. Laboratory costs	20–23 per cent of 6
8. Supervision	20 per cent of item (6)
9. Plant overheads	50 per cent of item (6)
10. Capital charges	10 per cent of the fixed capital
11. Insurance	1 per cent of the fixed capital
12. Local taxes	2 per cent of the fixed capital
13. Royalties	1 per cent of the fixed capital
Sub-total B	.....
Direct production costs A + B	.....
13. Sales expense	20–30 per cent of the direct
14. General overheads	production cost
15. Research and development	.....
Sub-total C	.....
Annual production cost = A + B + C =	.....
Production cost £/kg =	$\frac{\text{Annual production cost}}{\text{Annual production rate}}$

### 3.5.5. Variable Cost:

Table 13: Variable costs

Raw materials per year	\$29,98,800 x 12 = \$35 million
Miscellaneous	0.1x \$2864070= \$0.28 million
Utilities	Neglected
Shipping and Packaging	Neglected
Total	\$36 million

### 3.5.6. Fixed Costs:

Average salaries of Labors per year [55]= \$7973.4627

Table 14: Fixed costs

Maintenance	.05 x \$57281392=\$2.86 million
Operating Labor	\$7970
Lab Costs	0.2 x \$7973.4627=\$1590
Supervision	0.2 x \$7973.4627=\$1590
Plant Overheads	0.5 x \$7973.4627=\$3990
Capital Charges	0.1 x \$57281392=\$5.73 million
Insurance	0.01 x \$57281392=\$0.58 million
Taxes	0.02 x \$57281392=\$1.14 million
Royalties	0.01 x \$57281392=\$0.58 million
Total	\$10.9 million

Direct production cost = \$10.9 million+ \$36 million = \$47 million

Sales expenses, Overheads, Research and Development	0.2 x \$47 million = \$9.4 million
---	------------------------------------

Annual production cost = \$36 million +\$10.9 million +\$9.4 million = \$56.6 million

According to material balance calculation, the annual production rate of hydrogen =

5304.2kg/hr=45826560kg/yr

Production Cost = (\$56.6 million /yr) / (45826560kg/yr)

= \$1.23/kg

# Chapter-4

## Results and Discussions

First and foremost was the material balance, the members compared the results with the ones the members procured from FFC as their actual results to be as follow:

Table 15: Industrial and calculated results comparison

Stream	Compound	Nm <sup>3</sup> /h	Kmol/h	Composition (wet)
<b>5 Outlet Reformer</b>	<b>Hydrogen</b>	61308	2735.4107	0.3891
	<b>Nitrogen</b>	7720	344.4472	0.0490
	<b>Carbon Monoxide</b>	10639	474.6857	0.0675
	<b>Carbon Dioxide</b>	10058	448.7630	0.0638
	<b>Argon</b>	6	0.2677	3.8082E-05
	<b>Methane</b>	11588	517.0278	0.0736
	<b>Water</b>	56235	2509.0660	0.3569
		<b>157554</b>	<b>7029.6681</b>	<b>1</b>
<b>5 Outlet Reformer Calculated</b>	<b>Hydrogen</b>	58969	2631.0503	0.3795
	<b>Nitrogen</b>	7720	344.4472	0.0497
	<b>Carbon Monoxide</b>	10639	474.6857	0.0685
	<b>Carbon Dioxide</b>	9901	441.7580	0.0637
	<b>Argon</b>	6	0.2677	3.8617E-05
	<b>Methane</b>	11588	517.0278	0.0746
	<b>Water</b>	56548	2523.0313	0.3640
		<b>155371</b>	<b>6932.2681</b>	<b>1</b>

The composition for the dry basis is as follows:

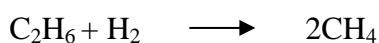
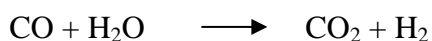
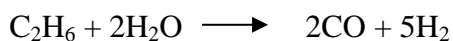
Table 16: Dry basis composition comparison

<b>Component Type</b>	<b>Composition Calculated (kmol/kmol)</b>	<b>Industrial Composition (kmol/kmol)</b>
<b>Hydrogen</b>	59.67%	61.18%
<b>Nitrogen</b>	7.81%	7.70%
<b>Carbon Monoxide</b>	10.77%	10.62%
<b>Carbon Dioxide</b>	10.02%	10.04%
<b>Argon</b>	0.01%	0.01%
<b>Methane</b>	11.73%	11.56%

The slight deviations present are because the members were explicitly asked to not include any ethane in the inlet stream to the reformer. This is not the case for the industrial conditions as there is a slight amount of ethane present in the inlet which undergoes its own ethane steam reforming and the produced carbon monoxide would then proceed with more water gas shift reaction.

It is however important to note that the methane exiting molar flow rate which is also termed as methane slippage is accurate to the industrial reading up to 7 decimal places which is a remarkable accuracy to achieve.

The reactions for ethane to undergo the process described above are as follow:



All these reactions would have had separate reaction kinetics and would have to be solved in the exact same method as discussed in the simulation part of the methodology, however this would have compounded the scope of the simulation to a large degree.



The conversions which the members achieved for the two reactions were:

Table 17: Conversion of reactions

<b>Conversion SMR %</b>	60.02759573
<b>Conversion WGS %</b>	38.86334905

Where SMR stands for steam methane reforming and WGS stands for water gas shift reaction.

The members move now to the energy balance results. The results varied to a certain degree with the simulation's results both of which are tabulated below:

Table 18: Calculated and simulated results

<b>kJ/h</b>	<b>Calculated</b>	<b>Simulated</b>	<b>% Error</b>
<b>Heat in to reformer</b>	$-8.762 \times 10^8$	$-8.99 \times 10^8$	2.6233
<b>Heat out of Reformer</b>	$-6.49 \times 10^8$	$-7.53 \times 10^8$	13.7596
<b>Heat in to Burner</b>	$-2.16 \times 10^8$	$-2.18 \times 10^8$	0.9538
<b>Heat out of Burner</b>	$-3.85 \times 10^8$	$-3.64 \times 10^8$	-5.6421

The calculated heat duty was found to be 40.44 Gcal/h whereas for the simulation it came out to be 35.02 Gcal/h. This was obtained by subtracting the heat in to the burner with the heat out of the burner for both cases. The industrial value was 35 Gcal/h which ensures the simulation results to be accurate up to the first decimal point.

The discrepancy of 5 Gcal/h was primarily due to the data coming from various sources, some of which were outdated, as opposed to ASPEN's itself which relied on

Peng-Robinson equations. Using the values for calculation from ASPEN Hysys, the members were able to reduce the error, the following are the values the members obtained:

Table 19: Error reduction

<b>kJ/h</b>	<b>Calculated</b>	<b>Simulated</b>	<b>% Error</b>
<b>Heat in to reformer</b>	$-8.762 \times 10^8$	$-8.99 \times 10^8$	2.6233
<b>Heat out of Reformer</b>	$-7.29 \times 10^8$	$-7.53 \times 10^8$	3.1420
<b>Heat in to Burner</b>	$-2.16 \times 10^8$	$-2.18 \times 10^8$	0.9538
<b>Heat out of Burner</b>	$-3.63 \times 10^8$	$-3.64 \times 10^8$	0.5533

These new values translated to a calculated heat duty of 35.04 Gcal/h with the same simulated value of 35.02 Gcal/h and the industrial value being 35 Gcal/h. The initial results of 97.213 % conversion were thus adjusted according to the simulation.

The simulation therefore assisted in the calculations which makes a very strong case for the accuracy of the simulation as it was able to catch the mistake and was able to minimize the error in the calculation which was caused by erroneous values for heat out of the reformer and out of the burner.

The members shall now discuss the results of the simulation. The screenshot below describes the conditions at which the simulation yielded the information for the streams:

	FEED	PRODUCTS	BURNFUEL	FLUE	
▶ Mole Flow kmol/hr	5459.32	7012.18	6292.23	6268.81	
▶ Mass Flow kg/hr	101610	101610	170838	170838	
▶ Volume Flow l/min	180532	1.23141e+06	71222.8	439479	
▶ Enthalpy MMBtu/hr	-852.861	315.622	-206.882	-1375.37	
▶ Mole Flow kmol/hr					
▶ AMMONIA					
▶ NITROGEN	344.47	344.47	470.135	470.135	
▶ HYDROGEN	79.91	2710.94	46.848		
▶ METHANE	1293.46	517.03	1857.87	11.71	
▶ ETHANE					
▶ OXYGEN			3715.75	trace	
▶ CO		474.69			
▶ CO2	140	441.74	201.27	2047.43	
▶ STEAM	3601.21	2523.04	0.178	3739.35	
▶ ARGON	0.267	0.267	0.178	0.178	

Figure 21: Table of conditions and compositions of simulation

This information was converted and then compared with the industrial data as can be seen below in the comparison of the outlet of the reformer.

Table 20: Calculated, simulated and industrial results comparison

<b>Composition</b>	<b>Calculated</b>	<b>Simulated</b>	<b>Industrial</b>
<b>Nitrogen</b>	344.45	344.47	344.45
<b>Hydrogen</b>	2631.05	2710.94	2735.41
<b>Methane</b>	517.02	517.03	517.03
<b>Ethane</b>	0	0	0
<b>Oxygen</b>	0	0	0
<b>Carbon monoxide</b>	474.69	474.69	474.69
<b>Carbon dioxide</b>	441.76	441.74	448.76
<b>Steam</b>	2523.03	2523.04	2509.07
<b>Argon</b>	0.268	0.267	0.268

For the control valves, the members plotted the variables across the percentage opening, keeping in mind the model the members used was equal percentage, and came across the following graph through the simulation.

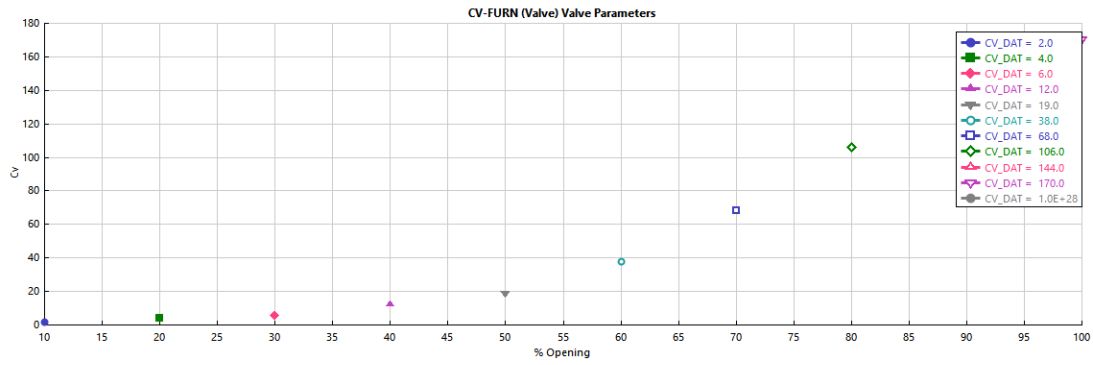


Figure 22: Cv and Percentage opening

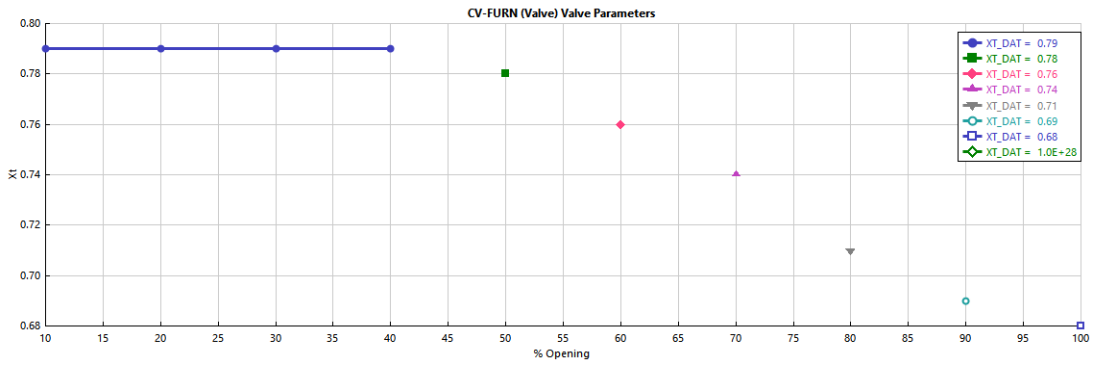


Figure 23: Xt and Percentage opening

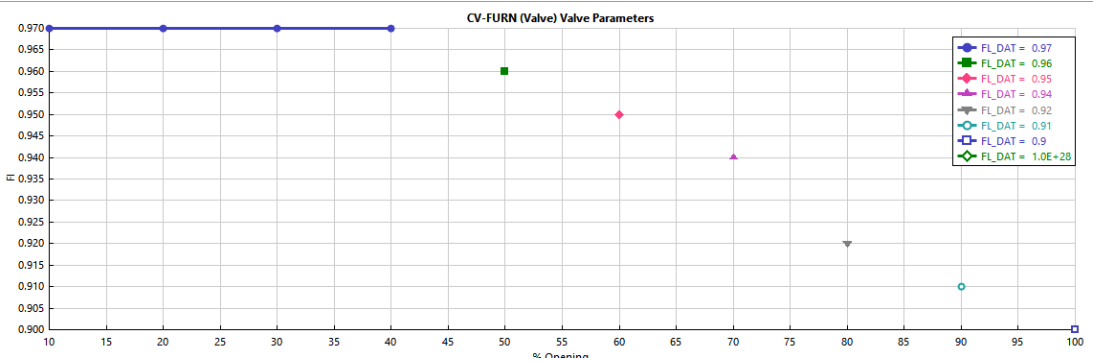


Figure 24: Fl and Percentage opening

Where Cv is the valve sizing coefficient, Xt is the related pressure drop ratio factor and Fl is the related liquid pressure recovery factor. Both the graphs were modeled on the same parameters as the information was not complete and had to resort to assumptions.

The results of the HAZOP provided with the following:

Table 21: HAZOP analysis of furnace

	<b>Guide Word</b>	<b>Parameter</b>	<b>Deviation</b>	<b>Cause</b>	<b>Consequences</b>
<b>1</b>	No	Temperature	No temperature	No fuel going in furnace	No combustion
<b>2</b>	Low	Temperature	Low temperature	Improper supply of fuel	Incomplete combustion
<b>3</b>	High	Temperature	High temperature	Higher supply of fuel	Fuel loss, Equipment damaged

Table 22: HAZOP analysis of reformer

	<b>Guide Word</b>	<b>Parameter</b>	<b>Deviation</b>	<b>Cause</b>	<b>Consequences</b>
<b>1</b>	No	Flow	No flow	No feed going to reformer	No reaction will take place
<b>2</b>	Low	Flow	Low flow	Lesser supply of feed	Incomplete reaction, Loss of energy
<b>3</b>	High	Flow	High flow	Higher supply of feed	High methane and steam slippage

The results of the costing provide with \$57281392 as the fixed capital with total raw material costs valuing at \$29,98,800/month. Variable costs amount to \$36272007 with fixed costs around \$12187438.46. Ultimately, the production costs value at \$1.26/kg.

# Conclusion

With the growing population of the world, the members as a collective species must sustain ourselves. Basic human needs include a source of nourishment and this project of ours is integral to the fertilizer industry, responsible for increasing the productivity of agriculture and horticulture.

The initial scope of the project was to simply simulate the primary reformer but the members went further and incorporated costing into it as well. This was primarily a learning experience for which expanded the theoretical knowledge with practicality. The project provided with a deeper understanding of engineering principles and how they shape the everyday lives. It instilled within the notion of such principles being applied universally and incorporated within a sense of responsibility as individuals who may practice and perhaps, one day, further these principles.

In the light of the shortage of Natural gas in Pakistan, it has become paramount for all fertilizer industries to shift their long term goal to using and finding alternative to natural gas as a fuel source and as a raw material for the firing of the furnace. One such alternative to finding the raw materials to manufacture syngas is coal gasification. Coal is abundant in Pakistan and utilizing this resource would ensure sustainability for years to come after the Mari gas reserves have been depleted, this is one of the more pressing matters in the near future.

There is also a global trend of using membrane reactors to ensure the approach to equilibrium can be minimized and more production can take place. The members reviewed such trends during the extensive literature review.

# References

- [1] Yu X, Tu S, Tung, Wang Z, Qi Y. Development of a microchannel reactor concerning steam reforming of methanol. *Chem Eng J* (2006).vol.32,pp.116-123
- [2] Peela NR, Mubayi A, Kunzru D. Steam reforming of ethanol over Rh/CeO<sub>2</sub>/Al<sub>2</sub>O<sub>3</sub> catalysts in a microchannel reactor. *Chem Eng J* (2011).vol.87,pp.167-578
- [3] Laosiripojana N, Assabumrungrat S. Methane steam reforming over Ni/Ce–ZrO<sub>2</sub> catalyst: Influences of Ce–ZrO<sub>2</sub> support on reactivity, resistance toward carbon formation, and intrinsic reaction kinetics. *Appl Catal A* (2005).vol.11,pp.200-290
- [4] Jeong JH, Lee JW, Seo DJ, Seo Y, Yoon WL, Lee DK, et al. Ru-doped Ni catalysts effective for the steam reforming of methane without the pre-reduction treatment with H<sub>2</sub>. *Appl Catal A* (2006).vol.6,pp.151-302
- [5] Xu J, Yeung CMY, Ni J, Meunier F, Acerbi N, Fowes M, et al. Methane steam reforming for hydrogen production using low water-ratios without carbon formation over ceria coated Ni catalysts. *Appl Catal A* (2008).vol.27,pp.119-345
- [6] Wu P, Li X, Ji S, Lang B, Habimana F, Li C. Steam reforming of methane to hydrogen over Ni-based metal monolith catalysts. *Catal Today* (2009).vol.6,pp.82-146
- [7] Le Valant A, Bion N, Can F, Duprez D, Epron F. Preparation and characterization of bimetallic Rh–Ni/Y<sub>2</sub>O<sub>3</sub>–Al<sub>2</sub>O<sub>3</sub> for hydrogen production by raw bioethanol steam reforming: influence of the addition of nickel
- [8] Hwang K-R, Lee C-B, Ryi S-K, Lee S-W, Park J-S. A multi-membrane reformer for the direct production of hydrogen via a steam-reforming reaction of methane. *Int J Hydrogen Energy* (2012).vol.37,pp.6601
- [9] Hwang K-R, Lee C-B, Lee S-W, Ryi S-K, Park J-S. Novel micro-channel methane reforming assisted combustion reaction for hydrogen production. *Int J Hydrogen Energy* (2011).vol.36,pp.473
- [10] Lee C-B, Lee S-W, Lee D-W, Ryi S-K, Park J-S, Kim S-H. Hydrogen production from methane steam reforming in combustion heat assisted novel microchannel reactor with catalytic stacking. *Ind Eng Chem Res* (2013).vol.52,pp.54-14049
- [11] W.W. Akers, D.P. Camp, Kinetics of methane–steam reforming, *AIChE J.*(1955) pp.471–475.

- [12] A.S. Al-Ubaid, S.S.E.H. Elnashaie, M. Abashar, Methane Conversion, Elsevier, New York, (1988).
- [13] L. Aparicio, Transient isotopic studies and microkinetic modelling of methane reforming over nickel catalysts, *J. Catal.* (1997).vol.165,pp.262–274.
- [14] N.M. Bodrov, L.O. Apelbaum, M.I. Temkin, Kinetics of the reactions of methane with steam on the surface of nickel, *Kinet. Catal.*(1964).vol.5,pp.696–705.
- [15] N.M. Bodrov, L.O. Apelbaum, M.I. Temkin, Kinetics of the reaction of methane with water vapour, catalysed nickel on a porous carrier, *Kinet. Catal.* (1967).vol.8,pp.821–828.
- [16] N.M. Bodrov, L.O. Apelbaum, M.I. Temkin, Kinetics of the reactions of methane with steam on the surface of nickel at 400–600\_C, *Kinet. Catal.* (1968).vol.9,pp.1065–1071.
- [17] J.C. De Deken, E.F. Devos, G.F. Froment, Steam Reforming of Natural Gas, *Chem. React. Eng. ACS Symp. Ser.*, (1982)pp.196.
- [18] A.E.C. Luna, A.M. Becerra, Kinetics of methane steam reforming on a Ni on alumina–titania catalyst, *React. Kinet. Catal. Lett.*(1997).vol.61,pp.369–374.
- [19] M.A. Soliman, M.A. Adris, A.S. Al-Ubaid, S.S.E.H. El-Nashaie, Intrinsic kinetics of nickel/calcium aluminate catalyst for methane steam reforming, *J. Chem. Tech. Biotechnol.*(1992).vol.55,pp.131–138.
- [20] J. Xu, G.F. Froment, Methane–steam reforming, methanation and water gas shift — I. Intrinsic kinetics, *AIChE J.*(1989).vol.35,pp.88–96.
- [21] M.V. Twigg, *Catalyst Handbook*, 2nd Edition, Wolfe Publishing Ltd., UK, (1989).
- [22] A.S. Al-Ubaid, Methane steam reforming activity, stability and characterization of nickel catalysts, Ph.D. Thesis, University of Notre Dame, IN, USA, (1984).
- [23] M.E. Agnelli, M.C. Demicheli, E.N. Ponzi, Catalytic deactivation on methane steam reforming catalysts: 2. Kinetics study, *Ind. Eng. Chem. Res.*(1987).vol.26, pp.1707–1713.
- [24] P.T. Quach, U.D. Rouleau, Kinetics of the methane–steam reaction over nickel catalyst in a continuous stirred tank reactor, *J. Appl. Chem. Biotechnol.*(1975) .vol.25,pp.445–459.
- [25] R. Kopsel, A. Richter, B. Meyer, Catalyst deactivation and kinetics of methane steam reforming, *Chem. Tech.*(1980).vol.32,pp.460.



- [26] D.W. Allen, E.R. Gerhard, M.R. Likins Jr., Kinetics of the methane–steam reaction, *Ind. Eng. Chem. Proc. Des. Dev.* (1975).vol.14,pp.256–259.
- [27] Toru Numaguchi, Kikuchi Katsutoshi, Intrinsic kinetics and design simulation in a complex reaction network: steam–methane reforming, *Chem. Eng. Sci.*(1988).vol.43,pp.2295–2301.
- [28] R.W. Blue, V.C.F. Holm, R.B. Regier, F. Edwin, L.F. Heckelsberg, Effect of granule size: in dehydrogenation and in hydrogen transfer reactions, *Ind. Eng. Chem.* (1952).vol.44,pp.2710–2715.
- [29] J.R.H. Ross, M.C.F. Steel, Mechanism of the steam reforming of methane over a coprecipitated nickel-alumina catalyst, *J. Chem. Soc., Faraday Trans.*(1972).vol.1,pp69.
- [31] Itoh, N.; Xu, W. and Haraya, K., Radial Mixing Diffusion of Hydrogen in a Packed- Bed Type of Palladium Membrane Reactor, *Ind. Eng. Chem. Res.*vol.33, pp.197 (1994).
- [32] Itoh, N., Simultaneous Operation of Reaction and Separation by a Membrane Reactor, *Studies in Surface Science and Catalysis*, by M. Misono, Y. Moro-oka and S. Kimura, Elsevier, New York (1990).vol.54, pp.268
- [34] Shu, J.; Grandjean, B.P.A. and Kaliaguine, S., Methane Steam Reforming in Asymmetric Pd- and Pd-Ag / Porous SS Membrane Reactors, *Applied Catalysis A: General*,(1994).vol.119, pp.305
- [35] Lewis, F.A., *The Palladium Hydrogen System*, Academic Press Inc., New York (1967).
- [36] Jemaa, N.; Shu, J.; Kaliaguine, S. and Grandjean, P. A., Thin Palladium Film Formation on Shot Peening Modified Porous Stainless Steel Substrates, *Ind. Eng. Chem. Res.* (1996).vol.35,pp.973
- [37] Lee AL. Internal reforming development for solid oxide fuel cells. Technical Report DOE/MC/22045e22364, US Department of Energy, Office of Scientific and Technical Information, Oak Ridge, TN.

- [38] Singhal SC. Solid oxide fuel cells: past, present and future. In: Irvine JTS, Connor P, editors. Solid oxide fuels cell: facts and figures. London: Springer-Verlag; 2013.vol.23,pp.1
- [39] Dicks AL. Advances in catalysis for internal reforming in high temperature fuel cells. J Power Sources (1998).vol.22,pp.71-111
- [40] Minh Nguyen Q. System technology for solid oxide fuel cells. In: Stolten D, Emonts B, editors. Fuel cell science and engineering: materials, process, systems and technology (2012).vol.2,pp. 963-1010.
- [41] Rostrup-Nielsen J, Christiansen LJ. Concepts in syngas manufacture, catalytic science series, Imperial College Press; 2011.vol.10
- [42] Clarke SH, Dicks AL, Pointon K, Smith TA, Swam A. Catalytic aspects of the steam reforming of hydrocarbons in internal reforming fuel cells. Catal Today (1997) .vol.23,pp.38-411
- [43] Rostrup-Nielsen JR. In: Anderson JR, Boudard M, editors. Catalysis, science and technology, Berlin: Springer Verlag; (1984) [Chapter 1].vol. 5
- [44] Rostrup-Nielsen JR, Rostrup-Nielsen T. Large-scale hydrogen production. Catech (2002).vol.9,pp.6-150
- [45] Nagel F, Schildhauer T, Biollaz S, Stucki S. Charge, mass and heat transfer interactions in solid oxide fuel cells operated with different fuel gases - a sensitivity analysis. J Power Sources (2008).vol.42,pp.129-184
- [46] Achenbach E, Riensche E. Methane/steam reforming kinetics for solid oxide fuel cells. J Power Sources (1994).vol.8,pp.52-283
- [47] Ahmed K, Foger K. Kinetics of internal steam reforming of methane on Ni/YSZ-based anodes for solid oxide fuel cells. Catal Today (2000).vol.87,pp.63-479
- [48] Lee AL, Zabransky RF, Huber WJ. Internal reforming development for solid oxide fuel cells. Ind Eng Chem Res (1990).vol.73,pp.29-766

- [49] Drescher I. Kinetik der Methan-Dampf-Reformierung. Diss RWTH Aachen; (1999).
- [50] Nagel F, Schildhauer T, Biollaz S, Stucki S. Charge, mass and heat transfer interactions in solid oxide fuel cells operated with different fuel gases - a sensitivity analysis. *J Power Sources* (2008).pp.184-129.
- [51] Levenspiel O. Chemical reaction engineering. 3rd ed. John Wiley & Sons; (1999)
- [52] Departamento de Físico-Química, Instituto de Química de São Carlos, Universidade de São Paulo, Av. Dr. Carlos Botelho, 1465, Cx. Postal 780, Phone: (016)273-9951, Fax: (016)273-9952, CEP:13560-970 - São Carlos, SP, Brazil
- [53] Departamento de Engenharia Química, Universidade Federal de São Carlos, Rod. Washington Luiz, km 235, Phone: (016)260-8264, Fax: (016)260-8266, CEP: 13565-905,
- [54] <https://ogra.org.pk/images/data/downloads/1441041000.pdf>
- [55] FFC financial statement report 2016, pp.142

# Appendices

## Appendix A.1

### Equilibrium Constants for the Methane–Steam Reaction at Various Temperatures



The equilibrium constants tabulated below are calculated from the following equation:

$$K_p = \exp(Z(Z(Z(0.2513Z - 0.3665) - 0.58101) + 27.1337) - 3.2770)$$

where  $Z = (1000/T) - 1$ , with  $T$  being the absolute temperature (Kelvin).  $K_p = K \times 10^n$  with  $K$  and  $n$  being listed below for temperatures over the range 200 to 1199°C.

Temperature/ °C	$K$					$n$
	+0°C	+1°C	+2°C	+3°C	+4°C	
200	2.1547	1.9201	1.7119	1.5269	1.3626	11
205	1.2166	1.0867	0.9712	0.8683	0.7767	11
210	6.9511	6.2236	5.5747	4.9957	4.4788	10
215	4.0172	3.6048	3.2361	2.9065	2.6115	10
220	2.3475	2.1110	1.8992	1.7094	1.5392	10
225	1.3865	1.2494	1.1264	1.0159	0.9166	10
230	8.2739	7.4713	6.7493	6.0994	5.5143	9
235	4.9872	4.5123	4.0842	3.6981	3.3498	9
240	3.0354	2.7516	2.4952	2.2636	2.0542	9
245	1.8649	1.6935	1.5387	1.3984	1.2713	9
250	1.1562	1.0519	0.9574	0.8716	0.7938	9
255	7.2322	6.5912	6.0091	5.4803	4.9996	8
260	4.5627	4.1653	3.8038	3.4749	3.1753	8

°C	+0°C	+1°C	+2°C	+3°C	+4°C	n
265	2.9026	2.6541	2.4277	2.2213	2.0331	8
270	1.8615	1.7048	1.5619	1.4314	1.3121	8
275	1.2032	1.1037	1.0127	0.9295	0.8533	8
280	7.8369	7.1994	6.6157	6.0811	5.5913	7
285	5.1425	4.7310	4.3538	4.0077	3.6902	7
290	3.3989	3.1314	2.8857	2.6601	2.4528	7
295	2.2623	2.0871	1.9261	1.7779	1.6416	7
300	1.5161	1.4006	1.2943	1.1963	1.1060	7
305	1.0229	0.9462	0.8755	0.8103	0.7501	7
310	6.9457	6.4332	5.9600	5.5231	5.1194	6
315	4.7464	4.4017	4.0830	3.7883	3.5157	6
320	3.2635	3.0302	2.8142	2.6142	2.4290	6
325	2.2575	2.0986	1.9513	1.8147	1.6881	6
330	1.5708	1.4619	1.3608	1.2670	1.1800	6
335	1.0992	1.0241	0.9544	0.8897	0.8295	6
340	7.7351	7.2149	6.7311	6.2811	5.8625	5
345	5.4729	5.1103	4.7728	4.4585	4.1657	5
350	3.8930	3.6389	3.4021	3.1814	2.9755	5
355	2.7836	2.6046	2.4376	2.2817	2.1363	5
360	2.0005	1.8737	1.7553	1.6447	1.5414	5
365	1.4448	1.3546	1.2702	1.1913	1.1176	5
370	1.0486	0.9840	0.9236	0.8671	0.8141	5
375	7.6460	7.1820	6.7474	6.3402	5.9587	4
380	5.6012	5.2661	4.9519	4.6573	4.3811	4
385	4.1219	3.8768	3.6506	3.4365	3.2355	4
390	3.0467	2.8695	2.7031	2.5467	2.3998	4
395	2.2618	2.1321	2.0101	1.8954	1.7876	4
400	1.6862	1.5908	1.5011	1.4166	1.3371	4
405	1.2623	1.1919	1.1256	1.0631	1.0043	4
410	9.4884	8.9662	8.4740	8.0101	7.5728	3
415	7.1605	6.7717	6.4050	6.0591	5.7327	3
420	5.4248	5.1342	4.8598	4.6009	4.3564	3
425	4.1255	3.9074	3.7014	3.5068	3.3229	3
430	3.1491	2.9849	2.8296	2.6828	2.5439	3
435	2.1426	2.2884	2.1709	2.0598	1.9546	3
440	1.8550	1.7608	1.6715	1.5871	1.5071	3
445	1.4313	1.3595	1.2915	1.2271	1.1660	3
450	1.1082	1.0533	1.0013	0.9520	0.9052	3

°C	+0°C	+1°C	+2°C	+3°C	+4°C	n
455	8.6088	8.1882	7.7891	7.4104	7.0510	2
460	6.7100	6.3863	6.0789	5.7871	5.5101	2
465	5.2469	4.9970	4.7596	4.5340	4.3196	2
470	4.1159	3.9223	3.7383	3.5634	3.3970	2
475	3.2388	3.0884	2.9453	2.8092	2.6797	2
480	2.5564	2.4392	2.3276	2.2213	2.1202	2
485	2.0239	1.9322	1.8449	1.7617	1.6825	2
490	1.6070	1.5351	1.4665	1.4012	1.3390	2
495	1.2797	1.2231	1.1692	1.1177	1.0687	2
500	1.0219	0.9773	0.9347	0.8941	0.8553	2
505	8.1834	7.8303	7.4933	7.1716	6.8645	1
510	6.5712	6.2911	6.0236	5.7680	5.5239	1
515	5.2907	5.0679	4.8550	4.6515	4.4570	1
520	4.2710	4.0933	3.9234	3.7608	3.6054	1
525	3.4568	3.3146	3.1786	3.0485	2.9240	1
530	2.8049	2.6909	2.5818	2.4774	2.3774	1
535	2.2816	2.1900	2.1022	2.0182	1.9377	1
540	1.8605	1.7867	1.7159	1.6481	1.5831	1
545	1.5208	1.4611	1.4039	1.3491	1.2965	1
550	1.2461	1.1977	1.1514	1.1069	1.0643	1
555	1.0233	0.9841	0.9464	0.9103	0.8756	1
560	8.4234	8.1040	7.7974	7.5031	7.2205	0
565	6.9492	6.6886	6.4384	6.1981	5.9673	0
570	5.7456	5.5326	5.3280	5.1313	4.9424	0
575	4.7608	4.5863	4.4185	4.2573	4.1023	0
580	3.9532	3.8099	3.6721	3.5396	3.4121	0
585	3.2895	3.1716	3.0581	2.9490	2.8440	0
590	2.7429	2.6457	2.5521	2.4620	2.3753	0
595	2.2918	2.2114	2.1340	2.0595	1.9878	0
600	1.9187	1.8521	1.7880	1.7263	1.6668	0
605	1.6094	1.5542	1.5010	1.4497	1.4003	0
610	1.3527	1.3068	1.2625	1.2198	1.1787	0
615	1.1390	1.1008	1.0639	1.0283	0.9940	0
620	9.6093	9.2900	8.9821	8.6850	8.3983	-1
625	8.1216	7.8547	7.5971	7.3484	7.1084	-1
630	6.8767	6.6531	6.4372	6.2287	6.0274	-1
635	5.8330	5.6453	5.4640	5.2889	5.1198	-1
640	4.9564	4.7986	4.6461	4.4988	4.3564	-1



°C	+0°C	+1°C	+2°C	+3°C	+4°C	n
645	4.2188	4.0859	3.9574	3.8332	3.7132	-1
650	3.5971	3.4849	3.3765	3.2716	3.1702	-1
655	3.0271	2.9773	2.8856	2.7969	2.7111	-1
660	2.6281	2.5478	2.4701	2.3950	2.3223	-1
665	2.2519	2.1838	2.1179	2.0541	1.9924	-1
670	1.9326	1.8748	1.8188	1.7646	1.7121	-1
675	1.6612	1.6120	1.5644	1.5182	1.4735	-1
680	1.4302	1.3882	1.3476	1.3082	1.2701	-1
685	1.2331	1.1973	1.1626	1.1290	1.0964	-1
690	1.0648	1.0342	1.0045	0.9758	0.9479	-1
695	9.2085	8.9464	8.6922	8.4458	8.2068	-2
700	7.9751	7.7503	7.5323	7.3209	7.1158	-2
705	6.9168	6.7238	6.5365	6.3548	6.1785	-2
710	6.0074	5.8414	5.6803	5.5240	5.3722	-2
715	5.2249	5.0819	4.9431	4.8084	4.6776	-2
720	4.5506	4.4272	4.3075	4.1912	4.0783	-2
725	3.9686	3.8621	3.7587	3.6582	3.5606	-2
730	3.4657	3.3736	3.2841	3.1971	3.1126	-2
735	3.0305	2.9508	2.8732	2.7979	2.7246	-2
740	2.6534	2.5842	2.5170	2.4516	2.3880	-2
745	2.3262	2.2681	2.2077	2.1509	2.0957	-2
750	2.0420	1.9897	1.9389	1.8895	1.8414	-2
755	1.7946	1.7492	1.7049	1.6618	1.6200	-2
760	1.5792	1.5396	1.5010	1.4634	1.4269	-2
765	1.3913	1.3567	1.3230	1.2902	1.2583	-2
770	1.2273	1.1970	1.1678	1.1389	1.1110	-2
775	1.0838	1.0573	1.0316	1.0065	0.9820	-2
780	9.5823	9.3504	9.1246	8.9047	8.6904	-3
785	8.4817	8.2784	8.0803	7.8873	7.6992	-3
790	7.5160	7.3375	7.1635	6.9939	6.8287	-3
795	6.6677	6.5107	6.3577	6.2086	6.0633	-3
800	5.9216	5.7835	5.6488	5.5175	5.3895	-3
805	5.2647	5.1430	5.0243	4.9086	4.7957	-3
810	4.6856	4.5783	4.4736	4.3715	4.2718	-3
815	4.1747	4.0799	3.9874	3.8972	3.8092	-3
820	3.7233	3.6395	3.5578	3.4780	3.4001	-3
825	3.3241	3.2500	3.1776	3.1070	3.0381	-3
830	2.9708	2.9051	2.8410	2.7784	2.7173	-3



°C	+0°C	+1°C	+2°C	+3°C	+4°C	n
835	2.6576	2.5994	2.5425	2.4870	2.4328	-3
840	2.3798	2.3281	2.2776	2.2283	2.1802	-3
845	2.1331	2.0872	2.0423	1.9985	1.9557	-3
850	1.9139	1.8730	1.8331	1.7941	1.7560	-3
855	1.7188	1.6824	1.6468	1.6121	1.5782	-3
860	1.5450	1.5126	1.4809	1.4499	1.4196	-3
865	1.3901	1.3611	1.3329	1.3052	1.2782	-3
870	1.2518	1.2260	1.2008	1.1761	1.1519	-3
875	1.1283	1.1053	1.0827	1.0606	1.0390	-3
880	1.0179	0.9973	0.9771	0.9574	0.9380	-3
885	9.1915	9.0067	8.8259	8.6490	8.4760	-4
890	8.3067	8.1410	7.9790	7.8204	7.6653	-4
895	7.5134	7.3649	7.2195	7.0772	6.9380	-4
900	6.8017	6.6683	6.5378	6.4100	6.2850	-4
905	6.1625	6.0427	5.9254	5.8105	5.6981	-4
910	5.5880	5.4803	5.3748	5.2714	5.1703	-4
915	5.0712	4.9742	4.8792	4.7862	4.6951	-4
920	4.6059	4.5185	4.4330	4.3491	4.2670	-4
925	4.1866	4.1078	4.0307	3.9551	3.8810	-4
930	3.8085	3.7374	3.6678	3.5995	3.5327	-4
935	3.4672	3.4030	3.3401	3.2785	3.2181	-4
940	3.1589	3.1009	3.0440	2.9883	2.9337	-4
945	2.8802	2.8277	2.7763	2.7259	2.6765	-4
950	2.6280	2.5805	2.5340	2.4883	2.4436	-4
955	2.3997	2.3567	2.3145	2.2732	2.2326	-4
960	2.1929	2.1539	2.1156	2.0781	2.0413	-4
965	2.0053	1.9699	1.9352	1.9012	1.8678	-4
970	1.8350	1.8029	1.7714	1.7405	1.7102	-4
975	1.6804	1.6512	1.6226	1.5945	1.5670	-4
980	1.5399	1.5134	1.4874	1.4618	1.4367	-4
985	1.4121	1.3880	1.3643	1.3411	1.3182	-4
990	1.2958	1.2739	1.2523	1.2311	1.2103	-4
995	1.1899	1.1699	1.1502	1.1309	1.1120	-4
1000	1.0934	1.0751	1.0572	1.0396	1.0223	-4
1005	1.0053	0.9887	0.9723	0.9562	0.9405	-4
1010	9.2498	9.0977	8.9483	8.8015	8.6574	-5
1015	8.5159	8.3769	8.2404	8.1063	7.9746	-5
1020	7.8453	7.7182	7.5934	7.4707	7.3503	-5



°C	+0°C	+1°C	+2°C	+3°C	+4°C	n
1025	7.2319	7.1157	7.0015	6.8893	6.7790	-5
1030	6.6707	6.5643	6.4597	6.3570	6.2580	-5
1035	6.1588	6.0593	5.9635	5.8694	5.7769	-5
1040	5.6860	5.5966	5.5088	5.4225	5.3376	-5
1045	5.2543	5.1723	5.0917	5.0126	4.9347	-5
1050	4.8582	4.7830	4.7091	4.6364	4.5649	-5
1055	4.4946	4.4256	4.3577	4.2909	4.2253	-5
1060	4.1607	4.0972	4.0348	3.9735	3.9131	-5
1065	3.8538	3.7954	3.7381	3.6816	3.6261	-5
1070	3.5715	3.5179	3.4651	3.4131	3.3621	-5
1075	3.3118	3.2624	3.2138	3.1660	3.1189	-5
1080	3.0727	3.0272	2.9824	2.9384	2.8950	-5
1085	2.8524	2.8104	2.7692	2.7286	2.6886	-5
1090	2.6493	2.6106	2.5726	2.5351	2.4983	-5
1095	2.4620	2.4263	2.3912	2.3567	2.3227	-5
1100	2.2892	2.2563	2.2238	2.1919	2.1605	-5
1105	2.1296	2.0992	2.0693	2.0398	2.0108	-5
1110	1.9822	1.9541	1.9264	1.8992	1.8723	-5
1115	1.8459	1.8199	1.7943	1.7691	1.7443	-5
1120	1.7199	1.6959	1.6722	1.6489	1.6259	-5
1125	1.6033	1.5810	1.5591	1.5375	1.5163	-5
1130	1.4953	1.4747	1.4544	1.4344	1.4147	-5
1135	1.3953	1.3762	1.3574	1.3389	1.3206	-5
1140	1.3026	1.2849	1.2675	1.2503	1.2334	-5
1145	1.2167	1.2003	1.1841	1.1682	1.1525	-5
1150	1.1370	1.1217	1.1067	1.0919	1.0773	-5
1155	1.0630	1.0488	1.0349	1.0211	1.0076	-5
1160	9.9427	9.8112	9.6817	9.5540	9.4282	-6
1165	9.3042	9.1821	9.0617	8.9430	8.8260	-6
1170	8.7108	8.5972	8.4852	8.3749	8.2661	-6
1175	8.1589	8.0532	7.9491	7.8464	7.7452	-6
1180	7.6454	7.5471	7.4501	7.3545	7.2603	-6
1185	7.1674	7.0759	6.9856	6.8966	6.8088	-6
1190	6.7223	6.6370	6.5529	6.4699	6.3882	-6
1195	6.3075	6.2280	6.1496	6.0723	5.9961	-6

## Appendix A.2

# Equilibrium Constants for the CO Conversion Reaction (Shift) at Various Temperatures



$$K_p = p_{\text{H}_2} p_{\text{CO}_2} / p_{\text{H}_2\text{O}} p_{\text{CO}}$$

The equilibrium constants tabulated below are calculated from the following equation:

$$K_p = \exp(Z(Z(0.63508 - 0.29353Z) + 4.1778) + 0.31688)$$

where  $Z = (1000/T) - 1$ , with  $T$  being the absolute temperature (Kelvin).  $K_p = K \times 10^n$  with  $K$  and  $n$  being listed below for temperatures over the range 200 to 1199°C.

Temperature/°C	K					n
	+0°C	+1°C	+2°C	+3°C	+4°C	
200	2.1082	2.0663	2.0254	1.9855	1.9464	2
205	1.9083	1.8711	1.8347	1.7991	1.7643	2
210	1.7304	1.6972	1.6648	1.6331	1.6021	2
215	1.5718	1.5421	1.5132	1.4849	1.4572	2
220	1.4301	1.4036	1.3777	1.3524	1.3276	2
225	1.3034	1.2797	1.2565	1.2338	1.2116	2
230	1.1899	1.1686	1.1478	1.1274	1.1075	2
235	1.0880	1.0689	1.0502	1.0319	1.0139	2
240	9.9638	9.7919	9.6236	9.4588	9.2973	1
245	9.1392	8.9843	8.8325	8.6839	8.5383	1
250	8.3956	8.2558	8.1188	7.9846	7.8530	1
255	7.7241	7.5977	7.4738	7.3524	7.2334	1
260	7.1167	7.0023	6.8901	6.7801	6.6723	1
265	6.5665	6.4628	6.3610	6.2613	6.1634	1
270	6.0674	5.9732	5.8808	5.7902	5.7012	1
275	5.6140	5.5284	5.4443	5.3619	5.2809	1

°C	+0°C	+1°C	+2°C	+3°C	+4°C	n
280	5.2015	5.1235	5.0470	4.9719	4.8981	1
285	4.8257	4.7546	4.6848	4.6163	4.5490	1
290	4.4829	4.4180	4.3543	4.2916	4.2301	1
295	4.1697	4.1104	4.0521	3.9949	3.9386	1
300	3.8833	3.8290	3.7756	3.7232	3.6716	1
305	3.6210	3.5712	3.5222	3.4741	3.4269	1
310	3.3804	3.3347	3.2898	3.2456	3.2022	1
315	3.1595	3.1175	3.0762	3.0356	2.9957	1
320	2.9564	2.9178	2.8798	2.8424	2.8057	1
325	2.7695	2.7339	2.6989	2.6645	2.6306	1
330	2.5973	2.5645	2.5322	2.5004	2.4691	1
335	2.4384	2.4081	2.3783	2.3489	2.3200	1
340	2.2916	2.2636	2.2360	2.2089	2.1822	1
345	2.1559	2.1300	2.1045	2.0794	2.0546	1
350	2.0303	2.0063	1.9826	1.9594	1.9364	1
355	1.9139	1.8916	1.8697	1.8481	1.8268	1
360	1.8059	1.7852	1.7649	1.7448	1.7251	1
365	1.7056	1.6864	1.6675	1.6489	1.6305	1
370	1.6124	1.5945	1.5769	1.5596	1.5425	1
375	1.5257	1.5090	1.4927	1.4765	1.4606	1
380	1.4449	1.4294	1.4141	1.3991	1.3842	1
385	1.3696	1.3551	1.3409	1.3268	1.3130	1
390	1.2993	1.2858	1.2725	1.2594	1.2464	1
395	1.2337	1.2211	1.2086	1.1964	1.1842	1
400	1.1723	1.1605	1.1489	1.1374	1.1261	1
405	1.1149	1.1039	1.0930	1.0822	1.0716	1
410	1.0611	1.0508	1.0406	1.0305	1.0205	1
415	1.0107	1.0010	0.9915	0.9820	0.9727	1
420	9.6345	9.5434	9.4536	9.3648	9.2772	0
425	9.1906	9.1051	9.0207	8.9373	8.8549	0
430	8.7735	8.6931	8.6138	8.5353	8.4578	0
435	8.3813	8.3057	8.2310	8.1572	8.0843	0
440	8.0122	7.9410	7.8707	7.8012	7.7325	0
445	7.6646	7.5975	7.5312	7.4657	7.4009	0
450	7.3369	7.2737	7.2111	7.1493	7.0883	0
455	7.0279	6.9682	6.9092	6.8508	6.7932	0
460	6.7362	6.6798	6.6241	6.5690	6.5145	0
465	6.4606	6.4074	6.3547	6.3026	6.2511	0

°C	+0°C	+1°C	+2°C	+3°C	+4°C	n
470	6.2002	6.1498	6.1000	6.0507	6.0020	0
475	5.9538	5.9061	5.8590	5.8124	5.7662	0
480	5.7206	5.6755	5.6308	5.5867	5.5430	0
485	5.4997	5.4570	5.4147	5.3728	5.3314	0
490	5.2904	5.2499	5.2098	5.1701	5.1308	0
495	5.0919	5.0534	5.0154	4.9777	4.9404	0
500	4.9035	4.8670	4.8309	4.7951	4.7597	0
505	4.7246	4.6899	4.6556	4.6216	4.5880	0
510	4.5547	4.5217	4.4891	4.4568	4.4248	0
515	4.3931	4.3617	4.3307	4.3000	4.2695	0
520	4.2394	4.2096	4.1800	4.1508	4.1218	0
525	4.0931	4.0647	4.0366	4.0087	3.9811	0
530	3.9538	3.9268	3.9000	3.8734	3.8471	0
535	3.8211	3.7953	3.7697	3.7444	3.7194	0
540	3.6945	3.6699	3.6456	3.6214	3.5975	0
545	3.5738	3.5503	3.5271	3.5041	3.4812	0
550	3.4586	3.4362	3.4140	3.3920	3.3702	0
555	3.3486	3.3272	3.3060	3.2850	3.2642	0
560	3.2435	3.2231	3.2028	3.1827	3.1628	0
565	3.1431	3.1235	3.1041	3.0849	3.0659	0
570	3.0470	3.0283	3.0098	2.9914	2.9732	0
575	2.9551	2.9372	2.9195	2.9019	2.8844	0
580	2.8671	2.8500	2.8330	2.8162	2.7995	0
585	2.7829	2.7665	2.7502	2.7340	2.7180	0
590	2.7022	2.6864	2.6708	2.6554	2.6400	0
595	2.6248	2.6097	2.5948	2.5799	2.5652	0
600	2.5506	2.5361	2.5218	2.5075	2.4934	0
605	2.4794	2.4655	2.4518	2.4381	2.4246	0
610	2.4111	2.3978	2.3846	2.3714	2.3584	0
615	2.3455	2.3327	2.3200	2.3074	2.2949	0
620	2.2825	2.2702	2.2580	2.2459	2.2339	0
625	2.2219	2.2101	2.1984	2.1867	2.1752	0
630	2.1637	2.1524	2.1411	2.1299	2.1188	0
635	2.1077	2.0968	2.0859	2.0752	2.0645	0
640	2.0539	2.0433	2.0329	2.0225	2.0122	0
645	2.0020	1.9919	1.9818	1.9718	1.9619	0
650	1.9521	1.9423	1.9327	1.9230	1.9135	0
655	1.9040	1.8946	1.8853	1.8760	1.8668	0

°C	+0°C	+1°C	+2°C	+3°C	+4°C	n
660	1.8577	1.8486	1.8396	1.8307	1.8218	0
665	1.8130	1.8043	1.7956	1.7870	1.7784	0
670	1.7699	1.7615	1.7532	1.7448	1.7366	0
675	1.7284	1.7203	1.7122	1.7042	1.6962	0
680	1.6883	1.6805	1.6727	1.6649	1.6573	0
685	1.6496	1.6420	1.6345	1.6270	1.6196	0
690	1.6123	1.6049	1.5977	1.5905	1.5833	0
695	1.5762	1.5691	1.5621	1.5551	1.5482	0
700	1.5413	1.5345	1.5277	1.5209	1.5143	0
705	1.5076	1.5010	1.4944	1.4879	1.4814	0
710	1.4750	1.4686	1.4623	1.4560	1.4497	0
715	1.4435	1.4373	1.4312	1.4251	1.4190	0
720	1.4130	1.4070	1.4011	1.3952	1.3893	0
725	1.3835	1.3777	1.3720	1.3663	1.3606	0
730	1.3550	1.3494	1.3438	1.3383	1.3328	0
735	1.3273	1.3219	1.3165	1.3111	1.3058	0
740	1.3005	1.2953	1.2900	1.2849	1.2797	0
745	1.2746	1.2695	1.2644	1.2594	1.2544	0
750	1.2494	1.2445	1.2396	1.2347	1.2299	0
755	1.2250	1.2203	1.2155	1.2108	1.2061	0
760	1.2014	1.1968	1.1922	1.1876	1.1830	0
765	1.1785	1.1740	1.1695	1.1651	1.1606	0
770	1.1562	1.1519	1.1475	1.1432	1.1389	0
775	1.1347	1.1304	1.1262	1.1220	1.1178	0
780	1.1137	1.1096	1.1055	1.1014	1.0974	0
785	1.0934	1.0894	1.0854	1.0814	1.0775	0
790	1.0736	1.0697	1.0659	1.0620	1.0582	0
795	1.0544	1.0506	1.0469	1.0432	1.0395	0
800	1.0358	1.0321	1.0285	1.0248	1.0212	0
805	1.0177	1.0141	1.0105	1.0070	1.0035	0
810	1.0000	0.9966	0.9931	0.9897	0.9863	0
815	9.8291	9.7954	9.7619	9.7286	9.6955	-1
820	9.6626	9.6298	9.5972	9.5648	9.5326	-1
825	9.5005	9.4686	9.4369	9.4054	9.3741	-1
830	9.3429	9.3118	9.2810	9.2503	9.2198	-1
835	9.1894	9.1592	9.1292	9.0993	9.0696	-1
840	9.0401	9.0107	8.9815	8.9524	8.9235	-1
845	8.8947	8.8661	8.8376	8.8093	8.7811	-1





°C	+0°C	+1°C	+2°C	+3°C	+4°C	n
850	8.7531	8.7252	8.6975	8.6699	8.6424	-1
855	8.6151	8.5880	8.5610	8.5341	8.5074	-1
860	8.4808	8.4543	8.4280	8.4018	8.3757	-1
865	8.3498	8.3240	8.2984	8.2729	8.2475	-1
870	8.2222	8.1971	8.1721	8.1472	8.1224	-1
875	8.0978	8.0733	8.0489	8.0247	8.0005	-1
880	7.9765	7.9526	7.9288	7.9052	7.8816	-1
885	7.8582	7.8349	7.8117	7.7886	7.7657	-1
890	7.7428	7.7201	7.6975	7.6750	7.6526	-1
895	7.6303	7.6081	7.5860	7.5641	7.5422	-1
900	7.5204	7.4988	7.4773	7.4558	7.4345	-1
905	7.4133	7.3921	7.3711	7.3502	7.3293	-1
910	7.3086	7.2880	7.2675	7.2470	7.2267	-1
915	7.2065	7.1863	7.1663	7.1463	7.1265	-1
920	7.1067	7.0871	7.0675	7.0480	7.0286	-1
925	7.0093	6.9901	6.9710	6.9519	6.9330	-1
930	6.9141	6.8954	6.8767	6.8581	6.8396	-1
935	6.8212	6.8028	6.7846	6.7664	6.7483	-1
940	6.7303	6.7124	6.6948	6.6768	6.6591	-1
945	6.6415	6.6240	6.6066	6.5892	6.5720	-1
950	6.5548	6.5376	6.5206	6.5036	6.4867	-1
955	6.4699	6.4532	6.4365	6.4199	6.4034	-1
960	6.3870	6.3706	6.3543	6.3381	6.3219	-1
965	6.3058	6.2898	6.2739	6.2580	6.2422	-1
970	6.2265	6.2108	6.1952	6.1797	6.1643	-1
975	6.1489	6.1335	6.1183	6.1031	6.0880	-1
980	6.0729	6.0579	6.0430	6.0281	6.0133	-1
985	5.9986	5.9839	5.9693	5.9548	5.9403	-1
990	5.9259	5.9115	5.8972	5.8830	5.8688	-1
995	5.8547	5.8406	5.8266	5.8127	5.7988	-1
1000	5.7850	5.7712	5.7575	5.7439	5.7303	-1
1005	5.7167	5.7032	5.6898	5.6765	5.6631	-1
1010	5.6499	5.6367	5.6236	5.6105	5.5974	-1
1015	5.5844	5.5715	5.5586	5.5458	5.5330	-1
1020	5.5203	5.5077	5.4950	5.4825	5.4700	-1
1025	5.4575	5.4451	5.4327	5.4204	5.4082	-1
1030	5.3960	5.3838	5.3717	5.3596	5.3476	-1
1035	5.3357	5.3237	5.3119	5.3000	5.2883	-1

°C	+0°C	+1°C	+2°C	+3°C	+4°C	n
1040	5.2765	5.2649	5.2532	5.2416	5.2301	-1
1045	5.2186	5.2072	5.1957	5.1844	5.1731	-1
1050	5.1618	5.1506	5.1394	5.1283	5.1172	-1
1055	5.1061	5.0951	5.0841	5.0732	5.0623	-1
1060	5.0515	5.0407	5.0300	5.0192	5.0086	-1
1065	4.9979	4.9874	4.9768	4.9663	4.9558	-1
1070	4.9454	4.9350	4.9247	4.9144	4.9041	-1
1075	4.8939	4.8837	4.8735	4.8634	4.8534	-1
1080	4.8433	4.8333	4.8234	4.8134	4.8036	-1
1085	4.7937	4.7839	4.7741	4.7644	4.7547	-1
1090	4.7450	4.7354	4.7258	4.7163	4.7067	-1
1095	4.6973	4.6878	4.6784	4.6690	4.6597	-1
1100	4.6504	4.6411	4.6319	4.6226	4.6135	-1
1150	4.6043	4.5952	4.5862	4.5771	4.5681	-1
1110	4.5591	4.5502	4.5413	4.5324	4.5236	-1
1115	4.5148	4.5060	4.4972	4.4885	4.4798	-1
1120	4.4712	4.4626	4.4540	4.4454	4.4369	-1
1125	4.4284	4.4199	4.4115	4.4031	4.3947	-1
1130	4.3863	4.3780	4.3697	4.3615	4.3532	-1
1135	4.3450	4.3369	4.3287	4.3206	4.3125	-1
1140	4.3045	4.2965	4.2885	4.2805	4.2725	-1
1145	4.2646	4.2567	4.2489	4.2410	4.2332	-1
1150	4.2254	4.2177	4.2100	4.2023	4.1946	-1
1155	4.1870	4.1793	4.1717	4.1642	4.1566	-1
1160	4.1491	4.1416	4.1342	4.1267	4.1193	-1
1165	4.1119	4.1046	4.0972	4.0899	4.0826	-1
1170	4.0754	4.0681	4.0609	4.0537	4.0466	-1
1175	4.0394	4.0323	4.0252	4.0182	4.0111	-1
1180	4.0041	3.9971	3.9901	3.9832	3.9762	-1
1185	3.9693	3.9625	3.9556	3.9488	3.9420	-1
1190	3.9352	3.9284	3.9217	3.9149	3.9082	-1
1195	3.9016	3.8949	3.8883	3.8817	3.8751	-1

## Nomenclature:

SMR	steam methane reforming
WGS	water gas shift reaction
MCR	micro-channel reactor
$X_{CH_4}$	methane conversion
$X_{CO_2}$	carbondioxide conversion
W	weight of catalyst (kg)
$F_i$	molar flow rate of component $i$ (kmol/s)
$r_{CH_4}$	rate of disappearance of methane in steam reforming (kmol/kg cat s)
$r_{CO_2}$	rate of formation of carbon dioxide in steam reforming (kmol/kg cat s)
$\dot{r}_{CH_4}$	rate of methane formation in reverse water gas shit reaction (kmol/kg cat s)
$\dot{r}_{CO_2}$	rate of carbon dioxide disappearance in reverse water gas shift reaction (kmol/kg cat s)
$a_i, \dot{a}_i$	correlation coefficients in Eqs. (3) and (7), respectively in Table 2 (kg cat s/kmol) <sup>-1</sup>
$b_i, \dot{b}_i$	correlation coefficients in Eqs. (4) and (8), respectively in Table 2 (kg cat s/kmol) <sup>-1</sup>
$P_i$	partial pressure of component $i$ (kPa)
$K_{p1}, K_{p3}$	equilibrium constant of reaction (1) and (3) respectively (kPa) <sup>2</sup>
$K_{p2}$	equilibrium constant of reaction (2)
$k_1, k_3$	reaction rate constants of reactions (1) and (3), respectively in Table 2 (kmol/kg cat s) (kPa) <sup>0.25</sup>
$k_2$	reaction rate constant of reaction (2) in Table 2 (kmol/kg cat s) (kPa)
R	reaction rate (kmol/kg cat s)
$E_i$	activation energy of reaction $i$ (kJ/mol)
$A_i$	pre-exponential factor of rate constant, $k_i$
$A(K_i)$	pre-exponential factor of rate constant, $K_i$
$\Delta H_{j,sa}$	enthalpy change of adsorption (kJ/mol)
R	universal gas constant (kJ/kmol/K)
T	temperature (K)
ATE	approach to equilibrium

$X_i$	conversion of component $i$
$Z$	length of the reactor (m)
$\rho_b$	density of the catalyst bed ( $\text{kg/m}^3$ )
$A$	cross sectional area ( $\text{m}^2$ )
$R_j$	rate of reaction $j$ ( $\text{kmol/kg}_{\text{cat}}/\text{h}$ )
$k^o$	reaction rate coefficient ( $\text{kmol/h/atm}$ )
$E_a$	activation energy ( $\text{kJ/mol}$ )
$K_{\text{eq}}$	equilibrium constant
$P_{\text{TOT}}$	total pressure ( $\text{N/m}^2$ )
$D_{\text{H}}$	diffusivity for hydrogen ( $\text{m}^2/\text{h}$ )
$t_m$	thickness of the membrane (m)
$C_r, C_s$	hydrogen concentrations ( $\text{kmol/m}^3$ )
$A_m$	area of membrane ( $\text{m}^2$ )
$d_m$	external diameter of the tubes (m)
$L$	length (m)
$u_i, v_i$	flow velocity of each component on the reaction and permeation side, respectively ( $\text{kmol/h}$ )
$r_i$	reaction rate ( $\text{kmol/m}^3/\text{h}$ )
SOFC	solid oxide fuel cell
$\Delta G_c$	gibbs free energy for carbon formation
$r_r, A_{rr}$	reaction rate of the steam reforming reaction
$F$	pre-exponential factor
$S/C$	steam to carbon ratio
YSZ	yttria-stabilized zirconia
$\Xi$	progress of reforming reaction variable
$T$	space time (s)
$M_r$	molecular mass ( $\text{g/mol}$ )
$\Delta H$	molar change in enthalpy ( $\text{kJ/kmol}$ )
$C_p$	heat capacity ( $\text{kJ/kmolC}^\circ$ )